

**SKB**

**TECHNICAL  
REPORT**

**93-09**

**Verification of the geostatistical  
inference code INFERENS, Version  
1.1, and demonstration using data  
from Finnsjön**

Joel Geier

Golder Geosystem AB, Uppsala

June 1993

**SVENSK KÄRNBRÄNSLEHANTERING AB**

*SWEDISH NUCLEAR FUEL AND WASTE MANAGEMENT CO*

BOX 5864 S-102 48 STOCKHOLM

TEL 08-665 28 00 TELEX 13108 SKB S

TELEFAX 08-661 57 19

VERIFICATION OF THE GEOSTATISTICAL INFERENCE CODE  
INFERENS VERSION 1.1 AND DEMONSTRATION USING DATA  
FROM FINNSJÖN

Joel Geier

Golder Geosystem AB, Uppsala

June 1993

This report concerns a study which was conducted for SKB. The conclusions and viewpoints presented in the report are those of the author(s) and do not necessarily coincide with those of the client.

Information on SKB technical reports from 1977-1978 (TR 121), 1979 (TR 79-28), 1980 (TR 80-26), 1981 (TR 81-17), 1982 (TR 82-28), 1983 (TR 83-77), 1984 (TR 85-01), 1985 (TR 85-20), 1986 (TR 86-31), 1987 (TR 87-33), 1988 (TR 88-32), 1989 (TR 89-40), 1990 (TR 90-46) and 1991 (TR 91-64) is available through SKB.

VERIFICATION OF THE GEOSTATISTICAL INFERENCE CODE  
INFERENS VERSION 1.1  
AND DEMONSTRATION USING DATA FROM FINNSJÖN

June 4, 1993

Joel Geier

Golder Geosystem AB  
Uppsala

Keywords: geohydrology, hydraulic conductivity, geostatistics, covariance models, semivariograms, estimation.

## ABSTRACT (ENGLISH)

This report describes preliminary verification and demonstration of the geostatistical inference code, INFERENS Version 1.1. This code performs regularization of packer test conductivities, and iterative generalized least-squares estimation (IGLSE) of nested covariance models and spatial trends for the regularized data. Cross-validation is used to assess the quality of the estimated models in terms of statistics for the kriging errors. The code includes a capability to generate synthetic datasets for a given configuration of packer tests; this capability can be used for verification exercises and numerical experiments to aid in the design of packer testing programs.

The report presents the results of a set of verification test cases. The test cases were designed to test the ability of INFERENS 1.1 to estimate the parameters of a variety of covariance models, with or without trends. This was done using synthetic datasets.

The verification exercises confirmed the functionality of the fitting algorithms, for intrinsic models with simple isotropic, simple horizontally isotropic, or nested isotropic covariances. The code also was successful in estimating models with spatial trends and simple isotropic or horizontally isotropic covariance. The more general forms of statistical anisotropy which are supported by INFERENS 1.1 were not adequately tested.

Verification of the fitting of more complex models, with nested anisotropic covariances, was not successful, primarily because the configuration and quantity of measurements in the synthetic datasets were not adequate for definition of the more complex models.

This report also describes an application of INFERENS 1.1 to the dataset from the Finnsjön site. The results are roughly similar to those obtained previously by Norman (1992a) using INFERENS 1.0, for the comparable cases. The actual numerical results are different, which may be due to changes in the fitting algorithms, and differences in how the lag pairs are divided into lag classes.

The demonstrations confirm the result previously obtained by Norman, that the fitted horizontally isotropic models are less good, in terms of their cross-validation statistics, than the corresponding isotropic models. The use of nested covariance models is demonstrated to give visually improved fits to the sample semivariograms, at both short and long lag distances. However, despite the good match to the semivariograms, the nested models obtained are not better than the simple models, in terms of cross-validation statistics.

These seemingly paradoxical results are explainable by the fact that the model fitting is performed by minimizing a weighted sum of the squared differences between the model covariance and the sample covariance, while the cross-validation statistics are calculated from the kriging errors using the fitted models. The optimum model in terms of cross-validation statistics is not necessarily coincident with the least-squares match to the sample covariance.

The use of direct fitting to the data pairs, rather than binned estimates (lag-class) of the semivariogram, in general is seen to yield poorer fits, as measured by the cross-validation statistics. This is interpreted as indicating that the direct-fitting approach is less robust. The relatively poor results achieved by direct fitting are problematic, since geostatistical inference using lag classes has been demonstrated to be highly sensitive to the arbitrary choice of lag classes.

**ABSTRACT (SWEDISH)**

Rapporten innehåller preliminär verifiering av samt demonstrationskörningar med den geostatistiska programkoden INFERENS, Version 1.1. Programmet utför regularisering, uppskalning, av konduktivitetsdata från borrhålstester. Vidare utförs iterativ, generaliserad minsta-kvadrat uppskattning (IGLSE) av nästlade kovariansmodeller och rumslig trend för de regulariserade data. S k "cross-validation" används för att beräkna kvalitén för de skattade modellerna uttryckt i statistik för felet vid kriging. Programkoden kan även generera syntetiska data för en given borrhålskonfiguration. Denna möjlighet kan utnyttjas för verifiering samt för numeriska experiment i samband med framtagning av borrhålsdesign.

Resultaten från ett antal verifieringsfall presenteras. Testfallen togs fram för att prova förmågan hos INFERENS 1.1 att skatta parametrar för ett antal olika kovariansmodeller, med och utan trend. Detta genomfördes med hjälp av syntetiska data.

Verifieringen bekräftade funktionen hos anpassningsalgoritmerna för enkla isotropa intrinsiska, för horisontellt isotropa samt för nästlade isotropa kovariansmodeller. Programmet lyckades också framgångsrikt skatta modeller med rumslig trend samt med isotrop eller horisontellt isotrop kovariansstruktur. Den mer generella form av statistisk anisotropi som implementerats i INFERENS 1.1 har ej verifierats inom projektet.

Verifiering av de mer komplexa statistiska modellerna, med nästlade anisotropa kovarianser, lyckades ej. Orsaken till detta är att konfigurationen av borrhål och antalet data ej var tillräckligt för dessa modeller.

Rapporten beskriver även praktisk tillämpning av INFERENS 1.1 på borrhålsdata från Finnsjön. Resultaten blir, för de jämförbara fallen, liknande de som erhöles i en tidigare studie, Norman (1992a), där INFERENS 1.0 användes. De numeriska värdena är dock olika vilket kan förklaras av förändringar i anpassningsalgoritmerna och skillnader vid indelningen i s k lag-klasser.

Tillämpningen bekräftar tidigare slutsatser av Norman, att de horisontellt isotropa kovariansmodellerna är sämre, när det gäller "cross-validation" statistik, än de motsvarande isotropa modellerna. De använda nästlade modellerna ger visuellt förbättrad passning när semivariogram betraktas, för både korta och långa s k lags. Trots denna bättre passning för semivariogram så är "cross-validation" statistiken sämre.

Detta resultat kan förefalla paradoxalt men kan förklaras av det faktum att modellanpassningen utförs genom minimering av en viktad kvadratsumma av skillnaden mellan modellkovariansen och den samplade kovariansen. "Cross-validation" statistiken baseras däremot på felet vid krigingsskattningen där de anpassade modellerna används. Således är inte den optimala statistiska modellen, baserad på "cross-validation" statistik, med nödvändighet sammanfallande med resultatet från minsta-kvadrat passning av samplade kovarianser.

Användandet av direkt anpassning mot data i stället för anpassning klassvis, lag-classes, vid konstruktion av semivariogram, ger generellt sämre resultat när det gäller "cross-validation" statistik. Detta kan tolkas som att den direkta anpassningsalgoritmen är mindre robust. Detta är relativt problematiskt eftersom geostatistisk passning med användande av s k lag-klasser har visat sig vara känsligt för den relativt godtyckliga indelningen i klasser.

## TABLE OF CONTENTS

## ABSTRACT

1.	INTRODUCTION	1
2.	FUNDAMENTAL CONCEPTS	3
2.1	Covariance models	3
2.2	Trend functions	5
2.3	Fitting algorithms	6
2.4	Cross-validation statistics	10
3.	VERIFICATION OF ALGORITHMS FOR MODEL ESTIMATION	12
3.1	Estimation of covariance models	14
3.2	Simultaneous estimation of covariance models and trend functions	36
4.	PRELIMINARY APPLICATION TO THE FINNSJÖN DATASET	43
4.1	Intrinsic models	44
4.2	Models with trends	55
5.	CONCLUSIONS	63
5.1	Verification cases	63
5.2	Demonstration using the Finnsjön dataset	64
5.3	Practicality of fitting algorithms and techniques	65
6.	ACKNOWLEDGEMENTS	68
7.	REFERENCES	69

List of Figures

- 2-1 Overview of INFERENS 1.1 model fitting algorithm
- 2-2 Lag class definition in INFERENS 1.1
  
- 3-1 2 x 2 borehole grid used for Test Cases 1-5, preliminary runs.
- 3-2 Input, simulated, and fitted models for simple isotropic covariance (2 x 2 grid)
  - a) Exponential covariance (testcase\_1e)
  - b) Spherical covariance (testcase\_1s)
- 3-3 4 x 4 borehole grid used to test fitting for larger data support
- 3-4 Input, simulated, and fitted models for simple isotropic covariance (4 x 4 grid)  
Exponential case
- 3-5 Input, simulated, and fitted models for horizontally anisotropic covariance (2 x 2 grid)
  - a) Exponential covariance (testcase\_2e)
  - b) Spherical covariance (testcase\_2s)
- 3-6 Input, simulated, and fitted models for nested isotropic covariance (2 x 2 grid)
  - a) Exponential covariance (testcase\_3e)
  - b) Spherical covariance (testcase\_3s)
- 3-7 Input, simulated, and fitted models for nested isotropic covariance (5 x 5 grid)
  - a) Exponential covariance (testcase\_3e)
  - b) Spherical covariance (testcase\_3s)
- 3-8 Input and fitted trends for horizontally isotropic covariance with potential-type trends
  - a) Exponential covariance (testcase\_1etf)
  - b) Spherical covariance (testcase\_1stf)
- 4-1 Finnsjön data and fitted simple, exponential isotropic, intrinsic model
  - a) Lag-class fitting (fiieil36)
  - b) Direct fitting (fiiein36)
- 4-2 Finnsjön data and fitted simple, spherical isotropic, intrinsic model
  - a) Lag-class fitting (fiisil36)
  - b) Direct fitting (fiisin36)
- 4-3 Finnsjön data and fitted exponential, horizontally isotropic, intrinsic model
  - a) Lag-class fitting (fiiehl36)
  - b) Direct fitting (fiiehn36)
- 4-4 Finnsjön data and fitted spherical, horizontally isotropic, intrinsic model
  - a) Lag-class fitting (fiishl36)
  - b) Direct fitting (fiishn36)
- 4-5 Finnsjön data and fitted nested, isotropic, intrinsic model
  - a) Exponential covariance (fiienl36)
  - b) Spherical covariance (fiisnl36)
- 4-6 Finnsjön data and fitted simple, exponential isotropic model with potential-type trend
  - a) Lag-class fitting (fipeil36)
  - b) Direct fitting (fipein36)
- 4-7 Finnsjön data and fitted simple, spherical isotropic model with potential-type trend
  - a) Lag-class fitting (fipsil36)
  - b) Direct fitting (fipsin36)

- 4-8 Finnsjön data and fitted exponential, horizontally isotropic model with potential-type trend
- 4-9 Finnsjön data and fitted spherical, horizontally isotropic model with potential-type trend
- 5-1 Intrahole and interhole data pairs



## 1. INTRODUCTION

This report describes preliminary verification and demonstration of the computer code INFERENS 1.1. This work was performed for Svensk Kärnbränslehantering AB (SKB) by Golder Geosystem AB (GGAB). Preliminary verification of INFERENS 1.1 was performed by generating synthetic datasets, and testing the ability of INFERENS 1.1 to deduce the models used to generate the synthetic datasets. The code was demonstrated by fitting a variety of models to conductivity data from the Finnsjön site.

INFERENS 1.1 was developed as a tool for estimating stochastic models based on borehole conductivity data. The code performs simultaneous, iterative generalized least-squares estimation (IGLSE) of nested covariance models (as defined in §2.1) and trend functions (as defined in §2.2) for packer test conductivity ( $K_p$ ) datasets.

INFERENS 1.1 is an extension and modification of INFERENS 1.0, which is described by Norman (1992a,b). The original code included modules to perform the following functions:

- Regularization of  $K_p$  data from overlapping and/or mismatched packer intervals, based on the steady-state formula of Moyes (1967).
- IGLSE of simple semivariogram models (isotropic or horizontally isotropic) and trend functions, using binned (lag-class) estimates of the sample semivariogram.
- Cross-validation (referred to as jackknifing) to estimate statistics for the kriging errors associated with a fitted semivariogram and trend model.
- Monte Carlo simulation of stochastic functions, based on the fitted models, to estimate the distribution of the cross-validation statistics in order to perform significance tests on the observed statistics.

An analysis of data from Finnsjön by Norman (1992a) using this code suggested that the relatively simple types of covariance models supported by INFERENS Version 1.0 may not be adequate for describing the covariance structure at an actual site. In that study it was found that, for every one of the fitted models, the hypothesis that the model was correct could be rejected at the 95% confidence level, based on the cross-validation statistics.

In other words, the models fitted using INFERENS 1.0 were not acceptable as kriging predictors of the hydraulic conductivity field, at a 95% confidence level. This finding, together with an observation of a possible nested covariance structure in the Finnsjön data, motivated further development of INFERENS to allow fitting of more complicated models.

Norman (1992a) also observed that the fitted models were strongly dependent on the arbitrary choice of lag-class divisions (bins) in the fitting process. This observation motivated further development of INFERENS to allow fitting without the need for arbitrarily defined lag classes.

A new version, INFERENS 1.1, was developed during 1992 to address the issues raised by the work of Norman (1992a). The capabilities of the original version were extended in INFERENS 1.1 to include:

- More general forms of geometric anisotropy for covariance models.
- Nested covariance models as defined in Section 2.1.
- Optional fitting directly to the data, rather than lag-class estimates.
- Optional constrained optimization, by holding a subset of the covariance model parameters fixed during optimization.
- Ability to generate synthetic datasets, based on an assumed covariance model, to facilitate verification of the fitting algorithm.

This document describes the results of running a set of verification test cases. The cases were designed to test the ability of the fitting algorithm to correctly estimate the parameters each of the different covariance models and trend functions supported by INFERENS 1.1. This document also describes an application of INFERENS 1.1 to the dataset from the Finnsjön site, and compares the results with those obtained using INFERENS 1.0 (Norman, 1992a).

## 2. FUNDAMENTAL CONCEPTS

The general form of stochastic function supported by INFERENS 1.1 is:

$$Y(x | p, \beta) = \tilde{Y}(x | p) + T(x | \beta) \quad (2-1)$$

where  $\tilde{Y}(x | p)$  is a stationary function with **nested covariance** defined by the parameter vector  $p$ , and the  $T(x | \beta)$  is a linear function of  $x$ , parameterized by the vector  $\beta$ , which is constructed as the sum of  $N_T$  trend functions. The terms in boldface are defined in the following sections.

### 2.1 Covariance models

A **nested covariance** is defined as a linear combination of ordinary covariances:

$$C(u_{ij}) = \sum_{n=1}^N \alpha_n C_n(u_{ij}) \quad (2-2)$$

where  $u_{ij} = x_i - x_j$  is the lag vector between two points, the  $\alpha_n$  are constant factors, and each **component model**  $C_n(u_{ij})$  is a spherical or exponential covariance model with geometrical anisotropy. In this report, it is assumed in general that  $\alpha_n = 1$ .<sup>1</sup>

Nested covariance models can be used to represent more complex correlation structures than can be represented with ordinary covariance models. In the simplest case this could be a field formed by superposition of two processes with isotropic covariance and contrasting ranges. This case was suggested as a result of the analysis of the Finnsjön data by Norman (1992a). More elaborate structures, *e.g.* the correlation structure which could result from three orthogonal sets of fracture zones, could be constructed by superposing anisotropic models.

Note that ordinary covariance models are a subset of nested covariance models (with  $N = 1$ ). Therefore statements made herein, concerning nested covariance models, will also pertain to the case of ordinary covariance models.

The **geometrical anisotropy** for the  $n$ th component model is defined in terms of a 3x3 anisotropy matrix  $G$  which maps each lag vector into an **isotropic covariance space**:

$$h_{nij} = G_n u_{ij} \quad (2-3)$$

where  $h_{nij}$  is the lag vector in the isotropic covariance space corresponding to the  $n$ th component model.

Each exponential or spherical covariance model is defined in the corresponding isotropic space, in the conventional manner.

---

<sup>1</sup> This entails no loss of generality, as the same effect can be represented by scaling the sills.

An exponential model is of the form:

$$C_n(\mathbf{u}_{ij}) = V_n e^{-\lambda_n h_{ij}} \quad (2-4)$$

A spherical model is of the form:

$$C_n(\mathbf{u}_{ij}) = \left\{ \begin{array}{ll} V_n \left( \frac{1}{2} \lambda_n^3 h_{ij}^3 - \frac{3}{2} \lambda_n h_{ij} \right) & 0 < h_{ij} < 1/\lambda_n \\ 0 & h_{ij} \geq 1/\lambda_n \end{array} \right\} \quad (2-5)$$

where:

$h_{ij} = |\mathbf{h}_{ij}|$  = the magnitude of the lag vector in the  $n$ th isotropic space.

$V_n$  = the variance of the  $n$ th component model.

$\lambda_n = 1/a_n$ , where  $a_n$  is the range of the  $n$ th component model.

The practical range for an exponential model is defined as  $a'_n = 3a_n$ .

A stochastic function with nested covariance can be constructed as a linear combination of mutually independent, component functions. This gives a straightforward way of simulating log conductivity fields with nested covariance, in INFERENS and HYDRASTAR, as the sum of independent turning bands simulations of the component models.

## 2.2 Trend functions

The general form of trend function supported by INFERENS 1.1 is:

$$T(x|\beta) = \sum_{i=1}^{N_T} T_i(x|\beta_i) \quad (2-6)$$

where the  $T_i(x|\beta_i)$ ,  $i = 1, 2, \dots, N_T$  are **component trend functions**. INFERENS 1.1 performs fitting with respect to the  $\beta_i$  on the following types of component trend functions:

Constant trend:

$$T_i(x) = \beta_i \quad (2-7)$$

Linear trend with respect to depth (the coordinate  $x_3$  or  $z$ ):

$$T_i(x|\beta_i) = -\beta_i x_3 \quad (2-8)$$

Logarithmic trend with respect to depth:

$$T_i(x|\beta_i) = -\beta_i \log(A+x_3) \quad (2-9)$$

where  $A$  is a constant.

Characteristic function defined with respect to a given domain  $D$ :

$$\tilde{Y} = \begin{cases} 1, & x \in D \\ 0, & x \notin D \end{cases} \quad (2-10)$$

The domain may be any particular one of the zones defined in the INFERENS task description file. Zones are defined as convex domains formed by the intersection of two or more half-spaces.

The linear trend is sometimes referred to as an exponential trend (Norman, 1992a) since in the case that  $Y(x) = \log_{10} K(x)$ , the resulting conductivity field is of the form:

$$K(x) = \tilde{K} \times 10^{-\beta_i x_3} \quad (2-11)$$

where  $\log_{10} \tilde{K} = \tilde{Y}$  is a random factor. The logarithmic trend is also referred to as a potential trend since, in the same case, the conductivity field is of the form:

$$K(x) = \tilde{K} \times (A+x_3)^{-\beta_i} \quad (2-12)$$

### 2.3 Fitting algorithm

INFERENS provides several alternative methods for estimating the vector of trend parameters,  $\beta$ , and the vector of covariance model parameters,  $p$ . All of the alternative methods are based on the method of **iterative generalized least-squares estimation**, or IGLSE. Several alternatives pertain to specific steps in the IGLSE algorithm:

- Direct or lag-class fitting.
- Constrained fitting and/or log-space fitting.

The basic IGLSE algorithm used in INFERENS 1.1 is as follows:

*Step 1:* Initial estimate of covariance model parameters  $p_{(i)}$  for iteration  $i = 1$ .

*Step 2:* Initial estimate of trend parameters  $\beta_{(i)}$  for iteration  $i = 1$ .

*Step 3:* Calculate the vector of residuals  $y$ :  $y_j = Y(x_j) - T(x_j | \beta_{(i)})$  for the  $j$ th data point,  $j = 1, 2, \dots, M$ .

*Step 4:* Nonlinear least squares estimation to optimize the covariance model for the residuals  $C_y(h | p_{(i)}) = E[y(x)y(x+h)]$ .

*Step 5:* Estimation of  $\beta_{(i+1)}$  by generalized least squares estimation (GLSE), assuming the covariance model  $C_y(h | p_{(i)})$ .

*Step 6:* Test for convergence with respect to  $\beta$ . If  $\|\beta_{(i+1)} - \beta_{(i)}\| > \epsilon_\beta$ , where  $\epsilon_\beta$  is a specified tolerance, then repeat Steps 3 - 6.

In the case where no trend functions are defined ( $N_T = 0$ ), the algorithm reduces to just Steps 1 and 4, *i.e.* non-linear least-squares estimation of  $p$ . In the non-trivial case  $N_T > 0$ , the initial estimate  $\beta_{(1)}$  is obtained by ordinary least squares regression (OLSR), which is equivalent to assuming, in this step, a pure nugget effect for the covariance model.<sup>2</sup>

Depending on the choice of **search method** (as specified in the task description file), INFERENS may be used to automatically run the IGLSE process repetitively, each time beginning with a different initial estimate  $p_{(i)}$ . If "no search" is specified, then IGLSE is performed just once, using the  $p_{(i)}$  which is specified in the task description file. If a **grid-based search** is specified, then the IGLSE estimation is performed repeatedly for different choices of  $p_{(i)}$ , which are taken from a uniformly-spaced grid in the  $N_p$  parameter space (Figure 2-1).

---

<sup>2</sup> This is a change from INFERENS 1.1, where  $\beta_{(1)}$  had to be supplied as input. It is difficult to imagine a case in which the user could supply a better initial guess of  $\beta$ , *a priori*, than the OLSR estimate. However, as seen from the results of verification runs given in Section 3.2, there may be a need to randomize  $\beta_{(1)}$  in certain cases.

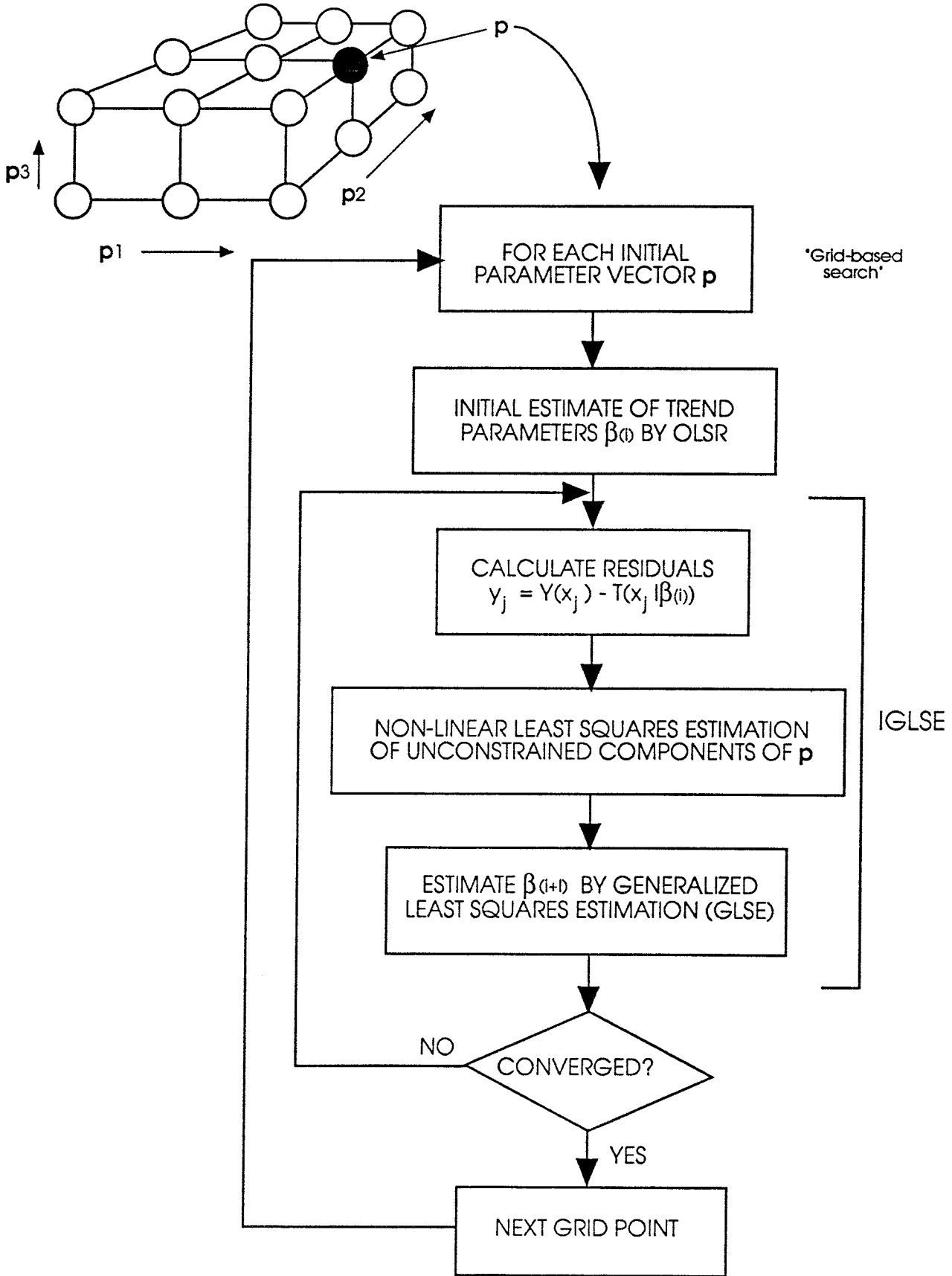


FIGURE 2-1  
 OVERVIEW OF INFERENS 1.1  
 MODEL FITTING ALGORITHM

The optimization of the covariance model parameters in Step 4 may be defined in terms minimizing either:

$$R_D = \sum_{ij} [C(u_{ij}) - y_i y_j]^2 \quad (2-13)$$

or

$$R_L = \sum_{ijk} w_{ijk} [\gamma(c_{ijk}) - \Gamma_{ijk}]^2 \quad (2-14)$$

where  $\gamma(u) = C(0) - C(u)$  is the semivariogram function, and  $w_{ijk}$ ,  $c_{ijk}$ , and  $\Gamma_{ijk}$  are, respectively, the assigned weight, the centroid, and the sample estimate of the semivariogram for the lag class  $L_{ijk}$ , as defined below. Optimizing with respect to  $R_D$  is termed **direct fitting**. Optimizing with respect to  $R_L$  is termed **lag-class fitting**.

A **lag class** is defined as a subset of the 3-D lag space. In INFERENS 1.1 the lag class divisions are defined in terms of spherical coordinates, as depicted in Figure 2-2. A given lag vector  $u$  is said to be a member of the lag class  $L_{ijk}$  if the components of  $u$  (in spherical coordinates) lie within the intervals:

$$\begin{aligned} r_{i-1} &\leq u_r < r_i \\ \theta_{j-1} &\leq u_\theta < \theta_j \\ \phi_{k-1} &\leq u_\phi < \phi_k \end{aligned} \quad (2-15)$$

where:

- $r_i$  = the  $i$ th radial lag class divisor,  $i = 0, 1, \dots, N_r$
- $\theta_j$  = the  $j$ th latitudinal lag class divisor,  $j = 0, 1, \dots, N_\theta$
- $\phi_k$  = the  $k$ th longitudinal lag class divisor,  $k = 0, 1, \dots, N_\phi$

The fitting in Step 3 may optionally be performed with respect to a subset of the covariance model parameters  $p$ , with the remaining components set to fixed values. This is referred to as **constrained fitting**. For example, a simple isotropic covariance model with parameters  $p_1 = V$  and  $p_2 = \lambda$  (the variance and inverse range, respectively) could be fitted with  $p_1$  set to some fixed value of  $V$ , so that only  $p_2$  would be allowed to vary during fitting.

The set of non-negativity constraints  $p_i > 0$ ,  $i = 1, 2, \dots, N_p$  can be applied by performing the fitting in log parameter space, *i.e.* by performing the optimization with respect to an auxiliary parameter vector  $q$  with components  $q_i = \log p_i$ . This method, referred to as **log-space fitting**, is generally recommended since negative  $p_i$  are implausible.<sup>3</sup>

---

<sup>3</sup> Log-space fitting is furthermore recommended as safer; there is a chance that a subprogram to calculate the value (or a partial derivative) of the objective function could produce a floating point error if passed a negative argument. Such an error could conceivably occur with ordinary fitting, but not with log-space fitting.



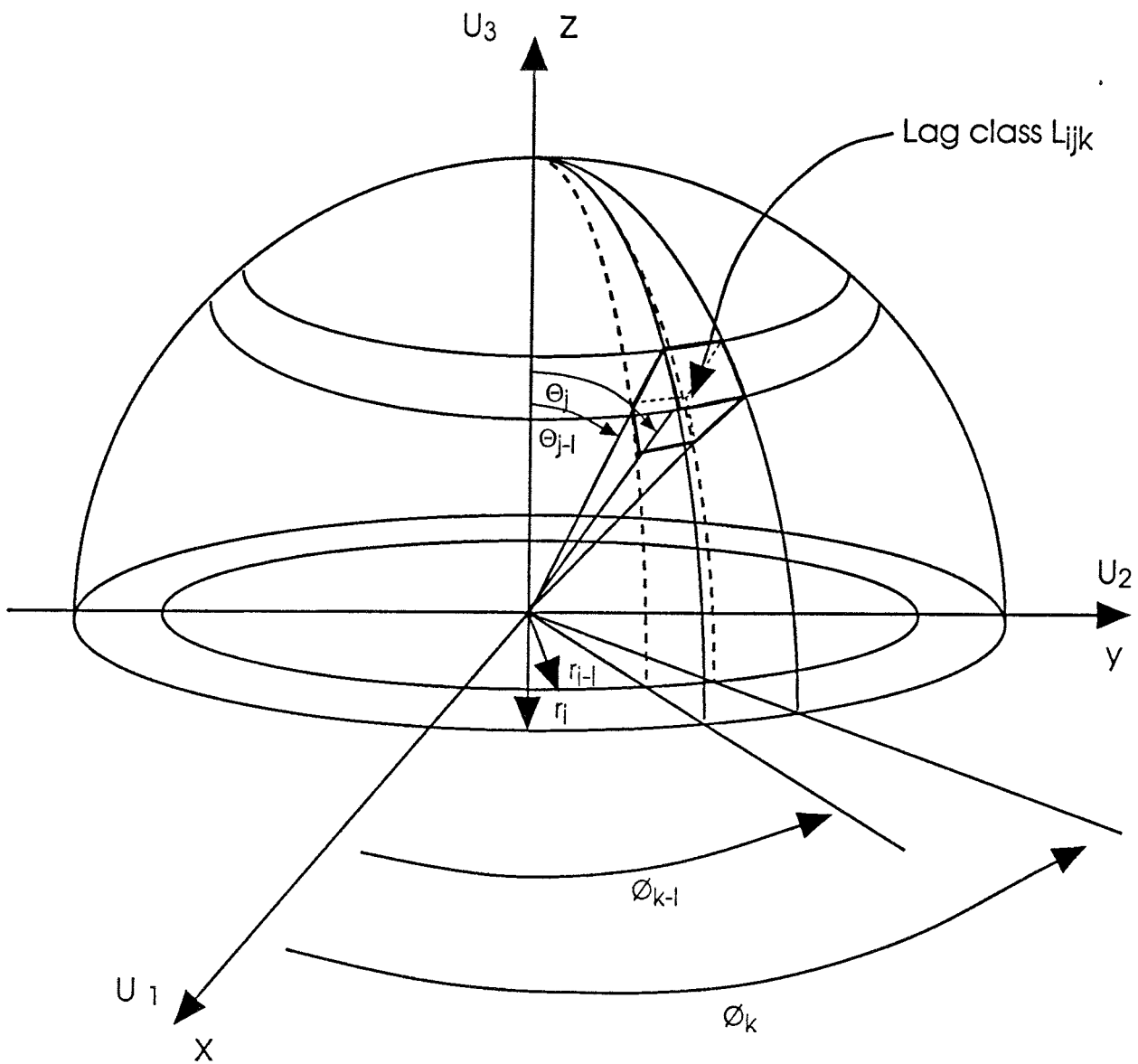


FIGURE 2-2  
LAG CLASS DEFINITION  
IN INFERENS 1.1

## 2.4 Cross-validation statistics

Cross-validation is a method for assessing the "goodness" of a given (presumably fitted) statistical model. The basic idea is to measure the goodness of the model by dividing the dataset into two portions, and then to use the first portion to predict the second portion of the dataset (Efron, 1982). A rather common approach (which is the one used in INFERENS) is the so-called "delete one" approach, in which the first portion of the dataset contains all the data points except one. The prediction errors can be analyzed in various ways to give a statistical assessment of the goodness of the model.

In the case of INFERENS, kriging is used to predict each deleted data point, in turn, based on the remainder of the dataset and the fitted covariance model. This gives a vector  $\epsilon$  of prediction errors (or "cross-validation errors," see Samper & Neumann, 1989), with components:

$$\epsilon_i = \hat{Y}(x_i) - Y(x_i) \quad (2-16)$$

where  $\hat{Y}(x_i)$  is the kriged estimate of  $Y(x_i)$ , for each point  $x_i$  in the dataset,  $i = 1, 2, \dots, M$ .

The vector of prediction errors  $\epsilon$  can be summarized in terms of various scalar statistics. The scalar statistics calculated by INFERENS are the **mean reduced error**, the **mean square reduced error**, and the **mean square error**, which are defined respectively as:

$$MRE = \frac{1}{M} \sum_{i=1}^M \hat{\epsilon}_i \quad (2-17)$$

$$MSRE = \frac{1}{M} \sum_{i=1}^M \hat{\epsilon}_i^2 \quad (2-18)$$

$$MSE = \frac{1}{M} \sum_{i=1}^M \epsilon_i^2 \quad (2-19)$$

where

$$\hat{\epsilon}_i = \frac{\epsilon_i}{\sqrt{E[\epsilon_i^2]}} \quad (2-20)$$

As discussed by Norman (1992a, p. 47), if the model is correct then  $MRE \approx 0$  and  $MSRE \approx 1$ .

In the limit as  $M \rightarrow \infty$ , these values should be obtained when the model is correct. However, in working with finite datasets, the values of MRE and MSRE will be randomly distributed around  $MRE = 0$  and  $MSRE = 1$ . In other words, for a finite dataset values of  $MSE \neq 0$  and  $MSRE \neq 1$  can be expected, even if the model is correct. In order to know if a given deviation from the expected values is significant, these distributions must be characterized.

INFERENS includes the possibility to estimate the distribution of MRE, MSRE, and MSE empirically, by the Monte Carlo method. This is done by generating random realizations of the fitted model, and, for each realization, calculating the measures MRE, MSRE, and MSE. This feature (referred to as the TESTJACK feature) produces estimates of the expected value, variance, and user-specified quantiles for the distributions of MRE, MSRE, and MSE. The significance of an observed value of any of these can be assessed by comparison with the empirical distribution.

### 3. VERIFICATION OF ALGORITHMS FOR MODEL ESTIMATION

INFERENS Version 1.1 includes the capability to generate a synthetic set of regularized, log conductivities, for a specified nested covariance model (or simple covariance model), with or without trend functions. To simulate a trend-free function  $\tilde{Y}(x)$  with nested covariance, independent realizations of the component functions  $\tilde{Y}_i(x)$  are generated using the turning bands (TUBA) method. These are summed to give a single realization of  $\tilde{Y}(x)$ . If trend functions are specified, these are added to the realization of  $\tilde{Y}(x)$  to give the function  $Y(x)$ .

This simulation capability is useful for verifying the performance of the IGLSE fitting algorithms, and for identifying the type of data support needed<sup>4</sup> to resolve the parameters of a given type of model. The simulator is also used during Monte Carlo estimation of the mean and variance of the cross-validation measures MRE, MSRE, and MSE.

Ideally the simulator itself should be properly verified, prior to using it to verify the INFERENS fitting algorithms. Verification of the simulator is not, however, a trivial exercise. The nested model simulation routines in INFERENS are based on the turning-bands simulation routines in HYDRASTAR, which were themselves the subject of a lengthy verification exercise (*Verification of HYDRASTAR*, SKB TR 91-27, Section 6.2.).

At the conclusion of that study, there remained questions regarding the significance of the observed deviations of the simulated sample variogram from the theoretical variogram. Some ideas have been suggested (Norman, personal communication, 1993) but could not be applied within the scope of this project. Verification of the simulator was therefore limited to visual comparisons.

The following notation is used for the sake of brevity, in discussing the results of the test cases:

$\gamma$	= the input (theoretical) semivariogram = $\gamma(u)$ .
$\Gamma$	= the sample variogram for the synthetic dataset = $\Gamma(u)$
$\hat{\gamma}$	= the fitted (estimated) semivariogram = $\hat{\gamma}(u)$ .

In the discussion of verification cases for exponential covariance models, the term "range" is understood to mean the practical range  $3/\lambda$ .

Five different test cases were devised for verifying the fitting of trendless models. The fitting of models with trends was verified by adding a trend function in each case, and performing IGLSE fitting.

---

<sup>4</sup> e.g. the total number of measurements, the number of boreholes, the spacing between boreholes, the inclinations of the boreholes, and the spacing between regularized measurements within the boreholes.

The basic procedure in each case was to:

1. Simulate a stochastic function on a regular grid of boreholes.
2. Estimate a covariance model from the synthetic data.
3. Calculate  $\Gamma$  and  $\hat{\gamma}$ .
4. Visually compare these with  $\gamma$ .

The verification cases were designed to test INFERENS 1.1 for a representative selection of the covariance models supported by the code, including simple isotropic models, simple horizontally anisotropic models, and several types of nested models, with and without superposed trend functions.

The set of verification cases is however not comprehensive. In particular, simple models with more general types of anisotropy (than horizontally isotropic) have not been tested individually, but only as components of complicated, nested models. If the ability of INFERENS to fit these complicated models were more clearly verified, there would be adequate confidence in INFERENS's ability to fit the components of these models. However, since the results of the most complicated verification cases are rather unclear, verification of the general anisotropic models, separately, is recommended.

The verification runs have been documented by software application memoranda (SAMs) which give the names and locations of input and output files, as well as other information which would be necessary for repeating or extending these verification runs. In the text which follows, the SAMs for each computer run are referenced by filing number (*e.g.* SAM 92-865-001).

### 3.1 Estimation of covariance models without trends

INFERENS 1.1 handles the relatively simple task of fitting a covariance model without trend functions, to regularized conductivity data. The fitting is performed by nonlinear least-squares regression. The algorithms for this simple task are applied in each step of the more complex task, of fitting a covariance model with trend functions. In the case of fitting an intrinsic model, this simple task constitutes the entire fitting problem.

Five different test cases were designed to check the performance of INFERENS 1.1 for fitting a covariance model without trends. The cases and results are described, in order of increasing complexity, in the following sections. Except as noted, all fitting was performed without use of lag classes (*i.e.* direct estimation) and in log-parameter space.

### 3.1.1. Test Case 1. Simple isotropic model

The purpose of Test Case 1 is to check that the fitting algorithms function correctly, for the simplest type of models supported by INFERENS 1.1.

The following input parameters were used for generating synthetic datasets:

Range = 75 m  
Sill = 1.5

Both exponential and spherical models were tested. The synthetic regularized data were generated for 3 m measurement spacings, on a 2 x 2 grid of 500 m long, vertical boreholes, with 100 m spacing between holes in the X and Y directions (Figure 3-1), giving a total of 664 data points. The following results were obtained:

Exponential covariance: testcase\_1e (SAM 92-865-009)

Fitted model:

Range = 35.0 m  
Sill = 1.52

Cross-validation statistics:

MRE = -0.00706  
MSRE<sup>1/2</sup> = 0.649  
MSE<sup>1/2</sup> = 0.401

Spherical covariance: testcase\_1s (SAM 92-865-010)

Fitted model:

Range = 62.7 m  
Sill = 1.15

Cross-validation statistics:

MRE = 0.00045  
MSRE<sup>1/2</sup> = 1.04  
MSE<sup>1/2</sup> = 0.301

Figures 3-2a,b show  $\gamma$ ,  $\Gamma$ , and  $\hat{\gamma}$  for these cases.

For the exponential case, the estimated variance is close to the input variance, but the (practical) range was underestimated by a factor of two. For the spherical case, the estimated range is close to the input range, but the estimated variance was 23% less than the input value. The cross-validation statistics for the exponential case are poor in comparison with the spherical model. Their significance should be checked by use of the TESTJACK feature as described in Section 2.4.

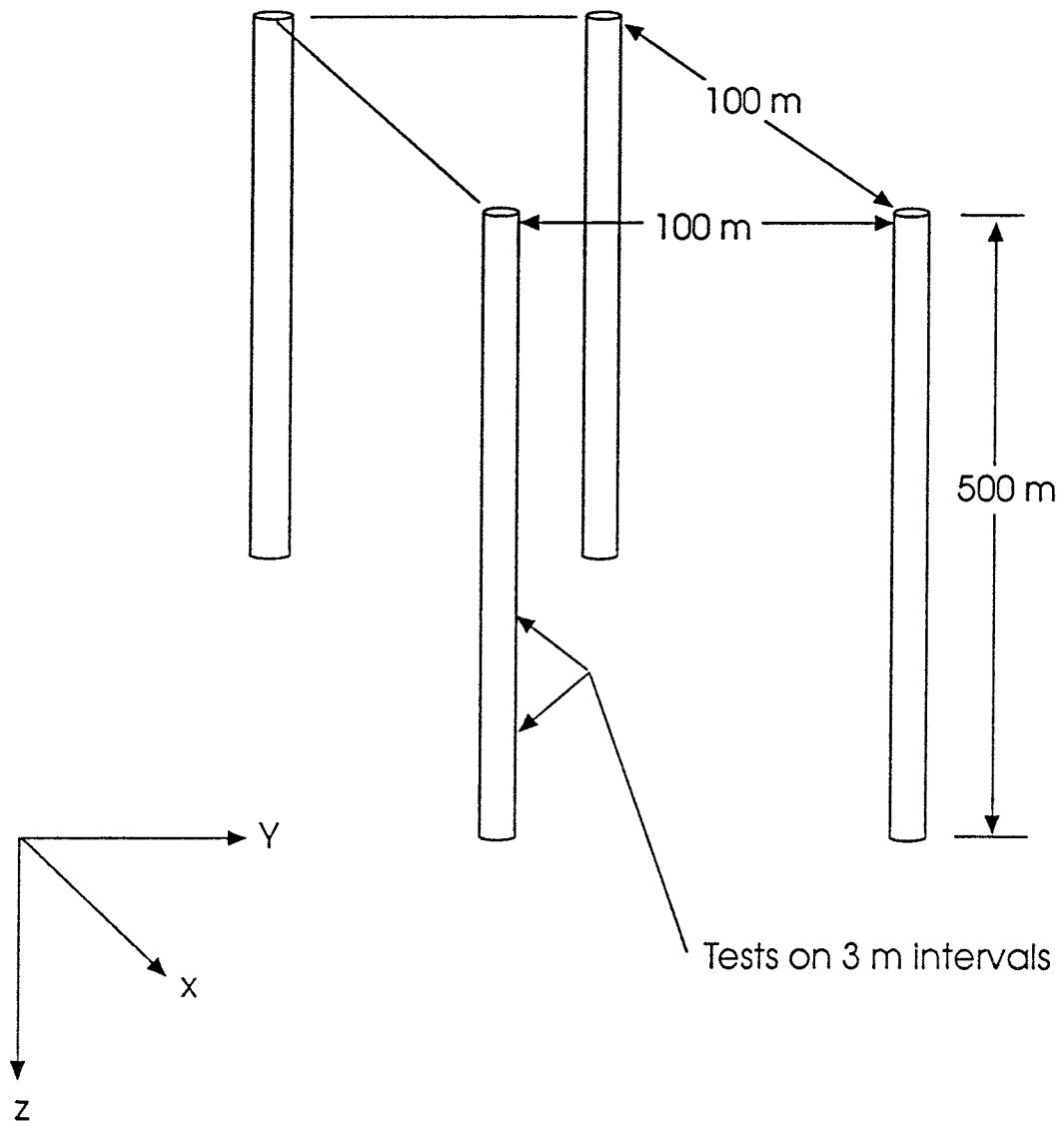
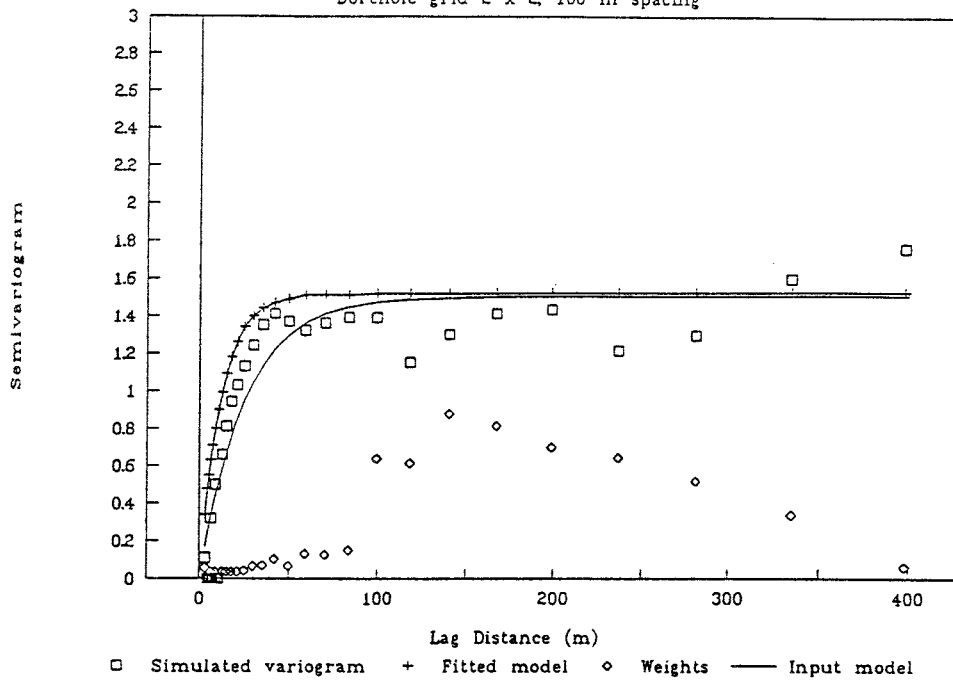


FIGURE 3-1  
2x2 BOREHOLE GRID



Case Name: testcase\_1e

Borehole grid 2 x 2, 100 m spacing



Case Name: testcase\_1s

Borehole grid 2 x 2, 100 m spacing

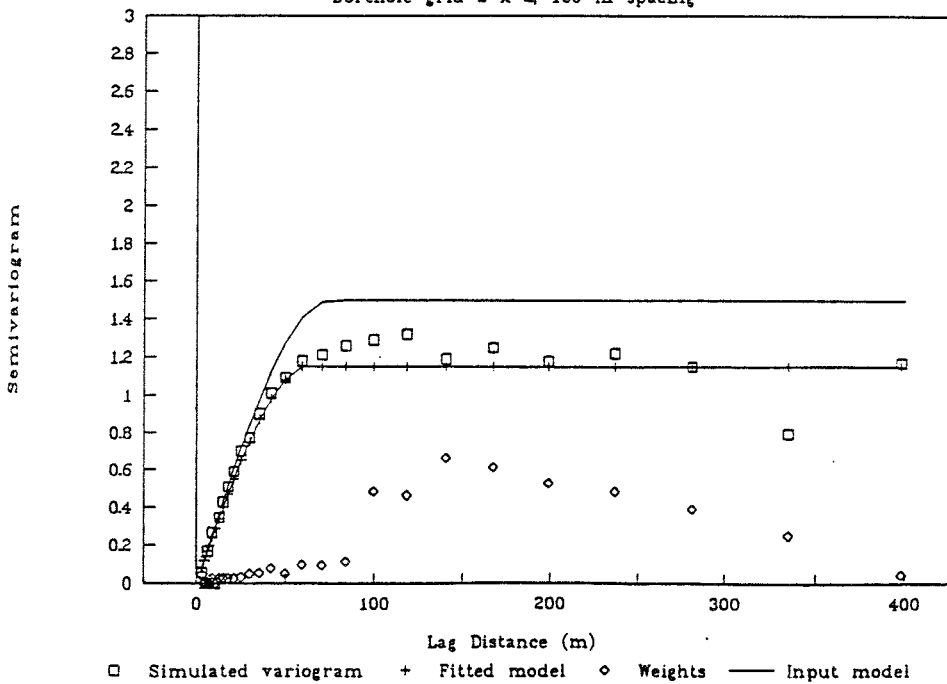


FIGURE 3-2a  
INPUT, SIMULATED SAMPLE,  
AND FITTED SEMIVARIOGRAM  
FOR TESTCASE\_1e (2x2 grid)

FIGURE 3-2b  
INPUT, SIMULATED SAMPLE,  
AND FITTED SEMIVARIOGRAM  
FOR TESTCASE\_1s (2x2 grid)

The plots suggest that a main cause of the discrepancy between input and fitted models is the difference between the sample  $\Gamma$  and the input  $\gamma$ . In both cases, the sum of the squared residuals (SSR) was less for the fitted values, than for the input values of the parameters. Thus the underestimate of the range is not because INFERENS failed to find a minimum SSR close to the input values in the parameter space. Rather, the parameter values which correspond to the least-squares criterion are different from the input values.

Possible causes for this discrepancy include:

- Error in the stochastic function simulation routines.
- Deficiencies in the minimum-SSR criterion as a criterion for estimating covariance models.
- Difference between model covariance and sample covariance for a finite realization.

The first of these seems unlikely since, for the simple covariance models considered here, the simulation routines are the same as in HYDRASTAR Version 1.1, and have been subjected to verification in this regard. A simulation of the exponential model for a larger borehole grid (see below) indicates that the match between  $\Gamma$  and  $\gamma$  improves with increasing data support.

The second possibility exists in theory because least-squares estimation disregards the correlation between values of the sample semivariogram (Samper and Neuman, 1989). The possibility was therefore explored that least-squares fitting gives systematically low estimates of the range, for exponential models. This was done by generating multiple realizations of the exponential model (using different seeds for the random number generator) and fitting the model to each realization.

For 10 unique realizations, the following were observed (SAM 92-865-017):

	Range (m)	Variance
Minimum	34.5	1.06
Maximum	88.3	1.76
Median	48.2	1.41
Mean	54.6	1.39
Standard dev.	16.9	0.26

It is seen that the results vary considerably between realizations, for the number and configuration of borehole measurements which were simulated. Judging from the median value, there may be a tendency to underestimate the true range by a factor of about 1.5. However, an experiment using a larger number of realizations is needed to determine whether this tendency is truly systematic.

The third cause, the effect of a finite realization, can be investigated by increasing the size of the data support (*i.e.* the number of synthetic boreholes). To investigate this, the test case for an exponential model was repeated using a 4 x 4 grid of synthetic boreholes (Figure 3-3).

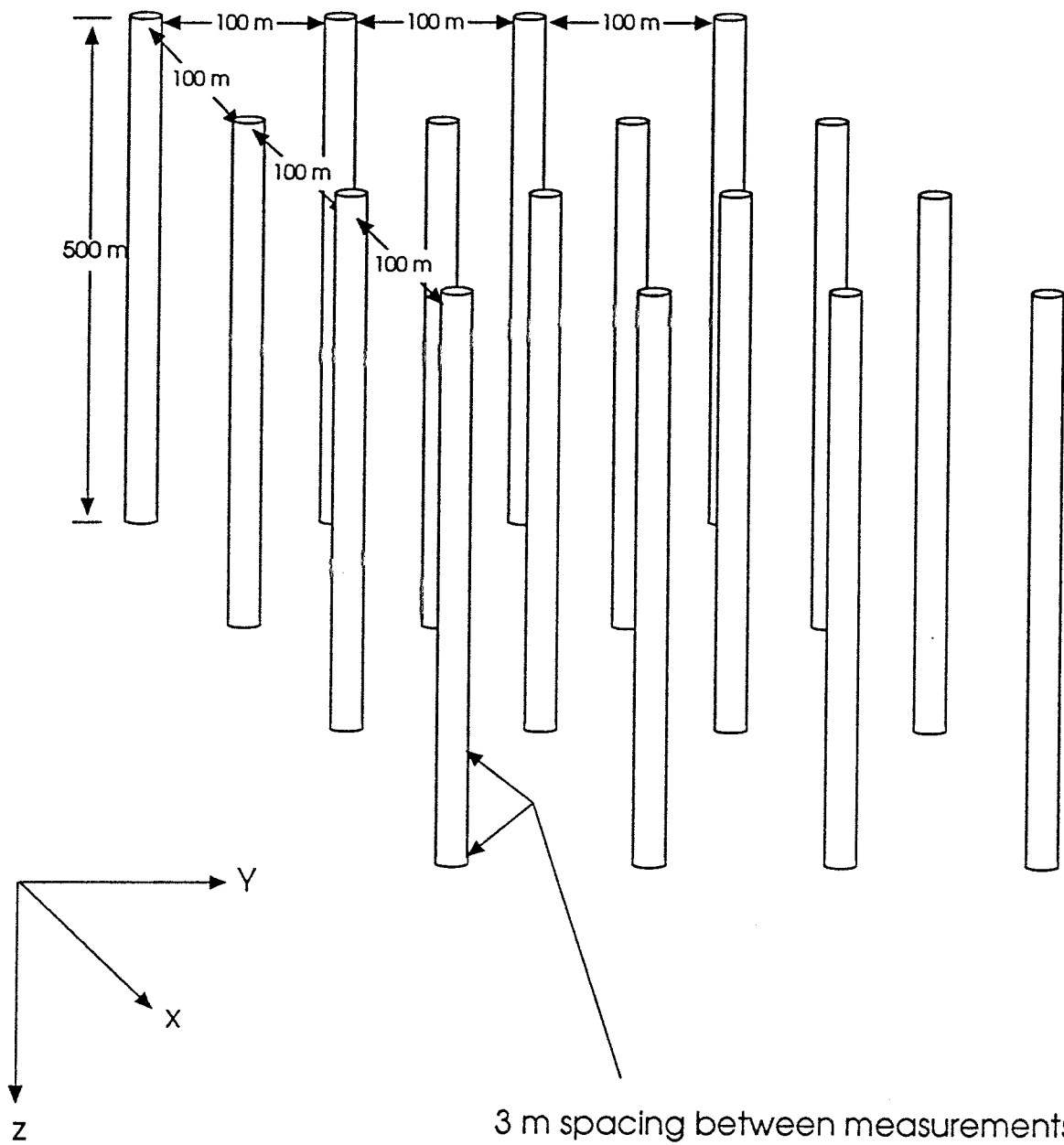


FIGURE 3-3  
4x4 GRID OF BOREHOLES

Exponential covariance: testcase\_1e (4 x 4 grid) (SAM 92-865-045)

Fitted model:

Range	= 59.5 m
Sill	= 1.40

Cross-validation statistics:

MRE	= -0.00965
MSRE <sup>1/2</sup>	= 0.902
MSE <sup>1/2</sup>	= 0.416

Figures 3-4 shows  $\gamma$ ,  $\Gamma$ , and  $\hat{\gamma}$  for this case. There is clearly an improvement in the match of  $\gamma$  and  $\Gamma$ , for the larger sample size. The estimated  $\hat{\gamma}$  is also closer to  $\gamma$ .

These results suggest that the main cause of the disagreement between  $\gamma$  and  $\hat{\gamma}$ , for the smaller borehole grid, is the limited size of the realization. In both cases the fitted variogram  $\hat{\gamma}$  is visually at least as good an approximation to  $\Gamma$  as is the input model  $\gamma$ . Thus the fitting algorithm, which is the main subject of this exercise, appears to function properly. The improvement of the match with increased data support indicates that both simulation and fitting routines are functioning properly for this type of model, and that the main issue is convergence of the semivariogram for the simulated dataset.

The question of whether the observed discrepancy between  $\gamma$  and  $\Gamma$  is significant (*i.e.* whether the simulated dataset is incorrectly generated) is a question of concern for HYDRASTAR verification, and deserves further consideration. Ideas regarding a significance test have been suggested (Norman, memorandum 93-02-17) but have not been implemented. This issue must be addressed before quantitative statements can be made regarding the veracity of the INFERENS fitting routines.

Case Name: testcase\_1e

Borehole grid 4 x 4 100 m spacing

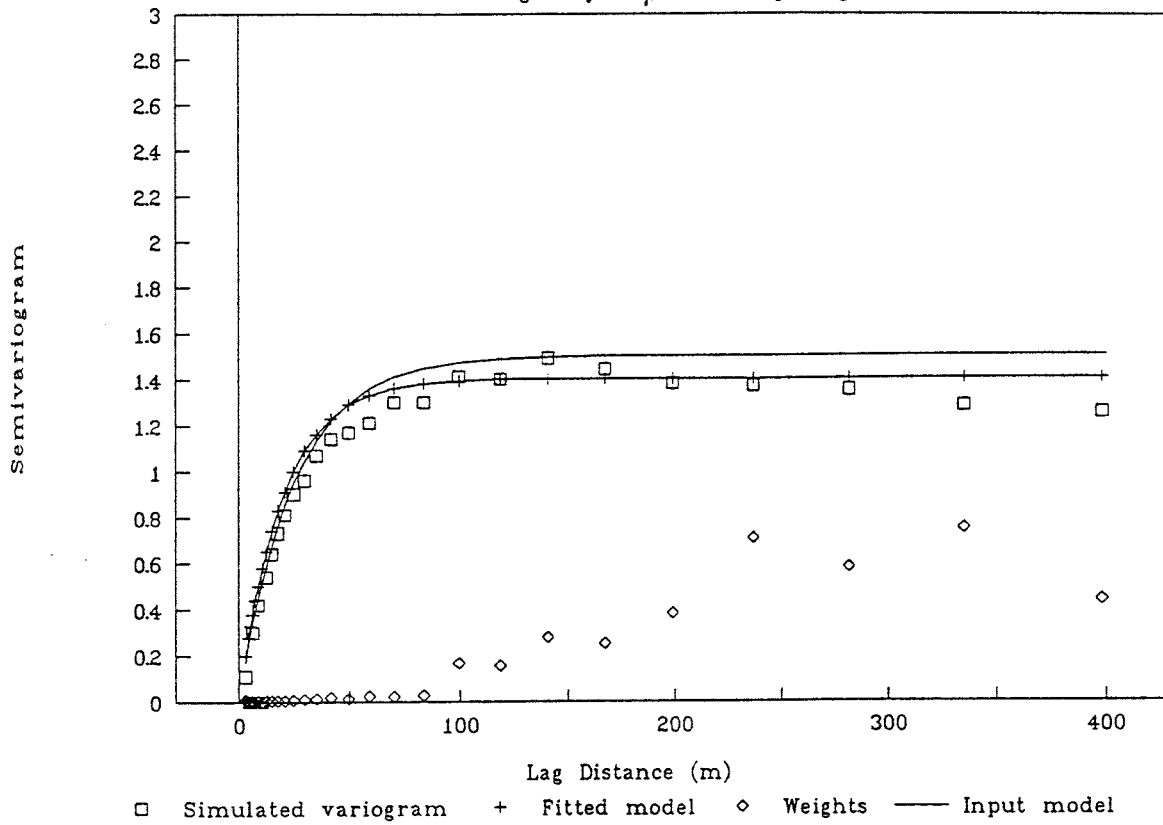


FIGURE 3-4  
INPUT, SIMULATED SAMPLE,  
AND FITTED SEMIVARIOGRAM  
FOR TESTCASE\_1e (4x4 grid)

### 3.1.2 Test Case 2. Simple horizontally isotropic model

The purposes of Test Case 2 are to check that (1) the horizontally isotropic type of model is handled correctly, and (2) the fitting algorithms function correctly for the components of the matrix of geometric anisotropy. The following input parameters were used for generating synthetic datasets:

$$\begin{aligned} \text{Range} &= 75 \text{ m} \\ \text{Sill} &= 1.5 \\ \mathbf{G} &= \begin{matrix} 0.2 & 0 & 0 \\ 0 & 0.2 & 0 \\ 0 & 0 & 5 \end{matrix} \end{aligned}$$

In standardized form, the range and anisotropy matrix become:

$$\begin{aligned} \text{Range} &= 128.2 \text{ m} \\ \mathbf{G} &= \begin{matrix} 0.342 & 0 & 0 \\ 0 & 0.342 & 0 \\ 0 & 0 & 8.55 \end{matrix} \end{aligned}$$

This model has relatively strong correlation in the horizontal direction. Possibly this covariance structure could be representative of a rock mass dominated by approximately horizontally extensive, highly conductive features.

Both exponential and spherical models were tested. The synthetic regularized data were generated for 3 m measurement spacings, on a 2 x 2 grid of 500 m long, vertical boreholes, with 100 m spacing between holes in the X and Y directions. The following results were obtained:

Exponential covariance: testcase 2e (SAM 92-865-011)

Fitted model (standardized form):

$$\begin{aligned} \text{Range} &= 138.4 \text{ m} \\ \text{Sill} &= 1.20 \\ \mathbf{G} &= \begin{matrix} 0.402 & 0 & 0 \\ 0 & 0.402 & 0 \\ 0 & 0 & 6.19 \end{matrix} \end{aligned}$$

Cross-validation statistics:

$$\begin{aligned} \text{MRE} &= 0.0363 \\ \text{MSRE}^{1/2} &= 1.33 \\ \text{MSE}^{1/2} &= 0.902 \end{aligned}$$

Spherical covariance model: testcase\_2s (SAM 92-865-012)

Fitted model (standardized form):

$$\begin{aligned} \text{Range} &= 98.9 \text{ m} \\ \text{Sill} &= 1.41 \\ \mathbf{G} &= \begin{matrix} 0.376 & 0 & 0 \\ 0 & 0.376 & 0 \\ 0 & 0 & 7.06 \end{matrix} \end{aligned}$$

Cross-validation statistics:

$$\begin{aligned} \text{MRE} &= -0.0185 \\ \text{MSRE}^{1/2} &= 0.917 \\ \text{MSE}^{1/2} &= 0.62 \end{aligned}$$

Comments

Figures 3-5a,b show  $\gamma$ ,  $\Gamma$ , and  $\hat{\gamma}$  for these two cases. In both cases, INFERENS produced model estimates which are close to the input models in terms of range and anisotropy. For the spherical case there is also good agreement in terms of variance. However, the estimated variance for the exponential case is 20% below the input model variance.

The good estimates of anisotropy are somewhat surprising in view of the type of data support, in which the non-vertical lags are represented only for distances close to the borehole spacing. Although the results are encouraging, further verification should be carried out using a simulated borehole configuration which gives better sampling of these lags (e.g. one with inclined holes).

The cross-validation statistics MRE and MSRE appear to be less good than for the isotropic models, in terms of the absolute deviations from the expected value of these statistics, *i.e.* in terms of  $|\text{MRE}|$  and  $|1 - \text{MSRE}^{1/2}|$ . However, in comparing among models one needs to take into account, for each model, the expected distributions of these statistics, for the particular sampling configuration, if one assumes that the model is correct. At a minimum estimates are needed of the variances  $V[\text{MRE}]$  and  $V[\text{MSRE}^{1/2}]$ .

Norman (1992a) demonstrated empirically, that the variances of cross-validation statistics for anisotropic models are approximately the same as for isotropic models, at least for the sampling configuration and parameter values which were treated in that study. However, the sampling configuration for this verification case is different from that considered by Norman (1992a), and furthermore the earlier study was restricted to fairly moderate anisotropy (a factor of 4).

In the present study, the dependency of  $V[\text{MRE}]$  and  $V[\text{MSRE}^{1/2}]$  on degree of anisotropy was explored by Monte Carlo simulation of the distributions of MRE and MSRE, for varying degrees of anisotropy. In all cases the underlying model was exponential, with  $V = 1.5$  and a (practical) range of 75, and 100 realizations were produced. The following results were obtained for four different cases, given in order of increasing anisotropy (SAM 92-865-052):

Run	$g_{33}/g_{11}$	$E[\text{MRE}]$	$V[\text{MRE}]^{1/2}$	$E[\text{MSRE}]$	$V[\text{MSRE}^{1/2}]^{1/2}$
4	1	0.0028	0.0081	0.991	0.052
2	8	0.0020	0.0171	0.994	0.048
1	25	0.0045	0.0210	0.998	0.041
3	1000	-0.0122	0.0438	0.991	0.045

It is interesting to note that  $V[\text{MRE}]$  increases with increasing anisotropy, whereas  $V[\text{MSRE}^{1/2}]$  is approximately invariant. Both  $V[\text{MRE}]$  and  $V[\text{MSRE}^{1/2}]$  are considerably larger than the corresponding estimates for models fitted to the Finnsjön dataset by Norman (1992a). This is presumably an effect of the smaller range and (perhaps more importantly) the smaller data support in the test case. The relative invariance of  $V[\text{MSRE}^{1/2}]$  between models was also observed by Norman. These results suggest that alternative models could just as well be compared on the basis of  $\text{MSRE}^{1/2}$  alone.

For Run 1, which is directly comparable to the case of exponential covariance (testcase\_2e), the 5% and 95% quantiles of the simulated distributions were:

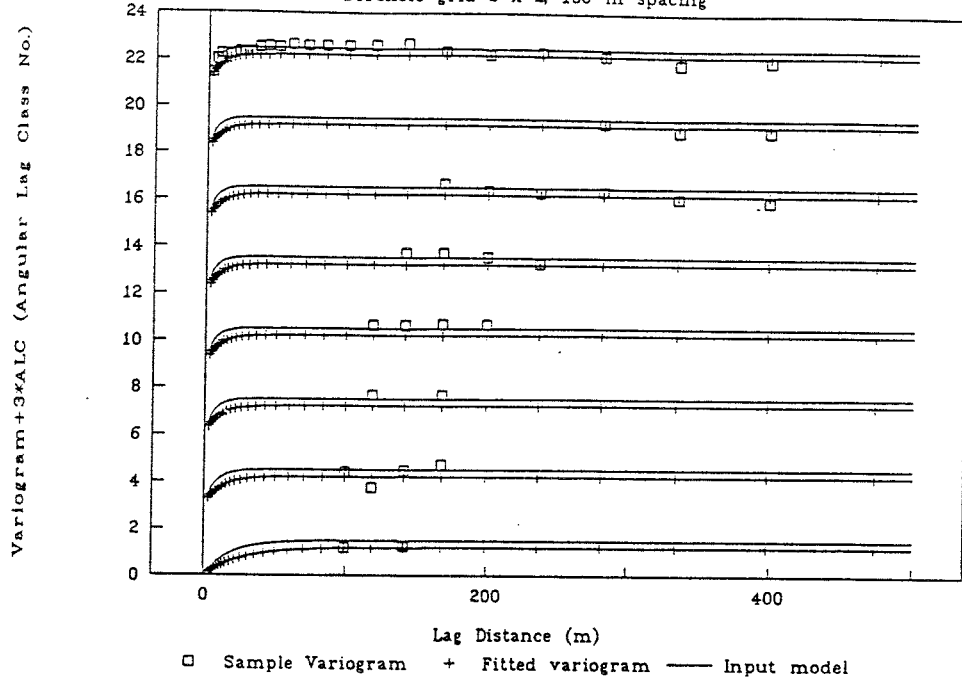
Quantile	MRE	$\text{MSRE}^{1/2}$
5%	-0.0280	0.922
95%	0.0425	1.06

On this basis the observed MRE of 0.0363 for the exponential case would not be rejected at the 90% confidence level (using a two-sided test), but the  $\text{MSRE}^{1/2}$  of 1.33 would be rejected at the same level. The observed MRE and  $\text{MSRE}^{1/2}$  for the spherical case would also be rejected at the 90% level, if the distributions of the jackknifing statistics in this case were assumed to be the same as for the exponential model. Thus the fitted models are unsatisfactory from a cross-validation point of view.



Case Name: testcase\_2e

Borehole grid 2 x 2, 100 m spacing



Case Name: testcase\_2s

Borehole grid 2 x 2, 100 m spacing

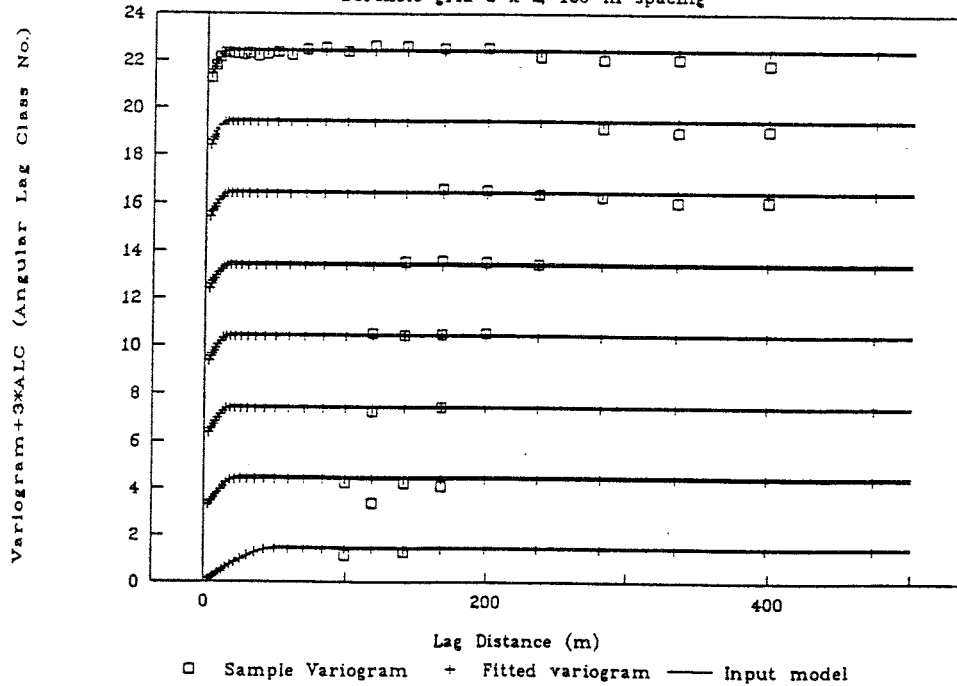


FIGURE 3-5a  
INPUT, SAMPLE, AND FITTED  
VARIOGRAMS FOR TESTCASE 2e

FIGURE 3-5b  
INPUT, SAMPLE, AND FITTED  
VARIOGRAMS FOR TESTCASE 2s

### 3.1.3 Test case 3. Nested isotropic models

Test Case 3 is a relatively simple form of nested model, designed to test for bugs (or other more fundamental problems) in the nested model simulation & estimation algorithms. The test case model is a summation of 3 simple covariance models (the submodels), each of which is isotropic.

The following input parameters were used for generating synthetic datasets:

Submodel 1	Range = 200 m
	Sill = 0.25
Submodel 2	Range = 100 m
	Sill = 0.5
Submodel 3	Range = 50 m
	Sill = 1.0

Both exponential and spherical submodels were tested. The synthetic regularized data were generated for 3 m measurement spacings, on a 2 x 2 grid of 500 m long, vertical boreholes, with 100 m spacing between holes in the X and Y directions. The following results were obtained:

Exponential covariance: testcase\_3e (SAM 92-865-013)

Fitted model:

Submodel 1	Range = 50.0 m
	Sill = 0.345
Submodel 2	Range = 50.1 m
	Sill = 0.516
Submodel 3	Range = 51.1 m
	Sill = 0.609

Cross-validation statistics:

MRE	= -0.0111
MSRE <sup>1/2</sup>	= 0.983
MSE <sup>1/2</sup>	= 0.504

Spherical covariance: testcase\_3s (SAM 92-865-014)

Submodel 1	Range = 64.1 m
	Sill = 0.241
Submodel 2	Range = 65.1 m
	Sill = 0.404
Submodel 3	Range = 67.5 m
	Sill = 0.677

Cross-validation statistics:

MRE	= 0.00695
MSRE <sup>1/2</sup>	= 1.12
MSE <sup>1/2</sup>	= 0.343

Figures 3-6a,b show  $\gamma$ ,  $\Gamma$ , and  $\hat{\gamma}$  for these cases. In both the exponential and the spherical cases, the nested conjugate-gradient fitting algorithm failed to resolve the separate submodels. Instead, all three estimated submodels, in each case, had nearly identical range estimates. In effect, a single isotropic model was fitted with a variance equal to the sum of the nested variances, and a range corresponding to the dominant range of the nested simulation. This result was obtained even though a grid-based search was used which ensured that each step in the search started with contrasting ranges for the submodels.

Judging from the sample semivariograms  $\gamma$  in Figures 3-6a,b, this size of sample does not give enough information for fitting the nested model. This is not surprising in view of the dependence, even for the simple isotropic models (Section 3.1.1), on the realization.

This test case was repeated for a 5 x 5 grid of vertical boreholes, with the same spacing between holes as before. The fitting was performed with respect to lag-class estimates of the semivariogram (*i.e.*,  $\gamma$  as shown in the figures) because fitting directly to the ca. 4000 data points in this case would have been too slow. The models thus estimated were:

Exponential covariance (SAM 92-865-041)

Fitted model:

Submodel 1	Range = 139.6 m
	Sill = 0.456
Submodel 2	Range = 87.0 m
	Sill = 0.976
Submodel 3	Range = 51.4 m
	Sill = 0.367

Spherical covariance (SAM 92-865-042)

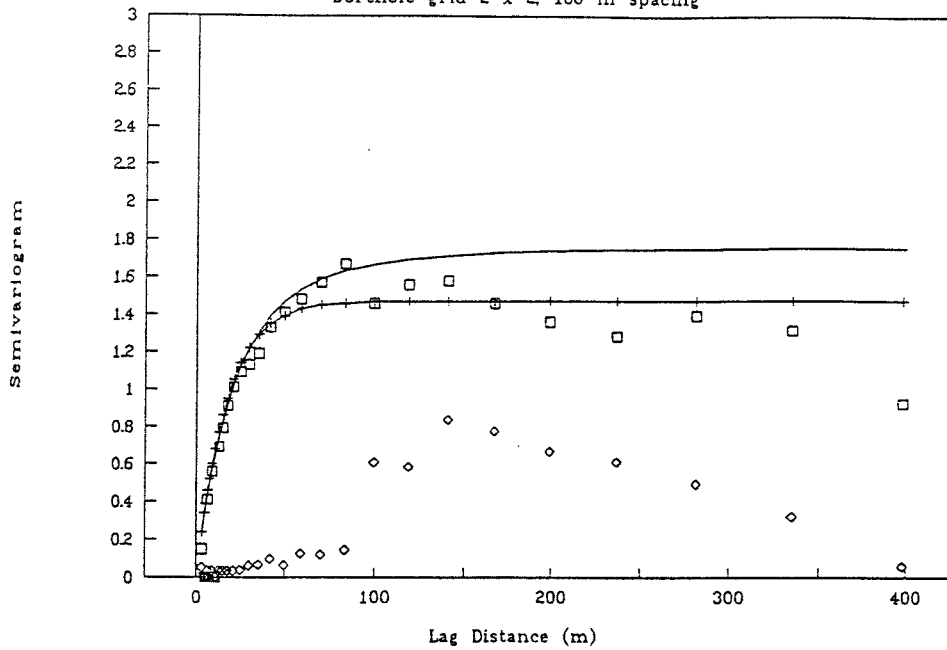
Submodel 1	Range = 143.8 m
	Sill = 0.854
Submodel 2	Range = 76.1 m
	Sill = 0.331
Submodel 3	Range = 15.9 m
	Sill = 0.626

Figures 3-7a,b show  $\gamma$ ,  $\Gamma$ , and  $\hat{\gamma}$  for these cases. Cross-validation failed in both cases because of a memory allocation failure (The dimension of the array RDYN apparently needed to be increased).

In both cases, three submodels are distinguished, although these are not the same as the input submodels. In the exponential case,  $\hat{\gamma}$  is a moderately good approximation to both  $\gamma$  and  $\Gamma$ . In the spherical case, there is a noticeable discrepancy in the lag range from 10 to 50 m, but the fit of  $\hat{\gamma}$  to  $\Gamma$  at medium and long lags is visually good.

Case Name: testcase\_3e

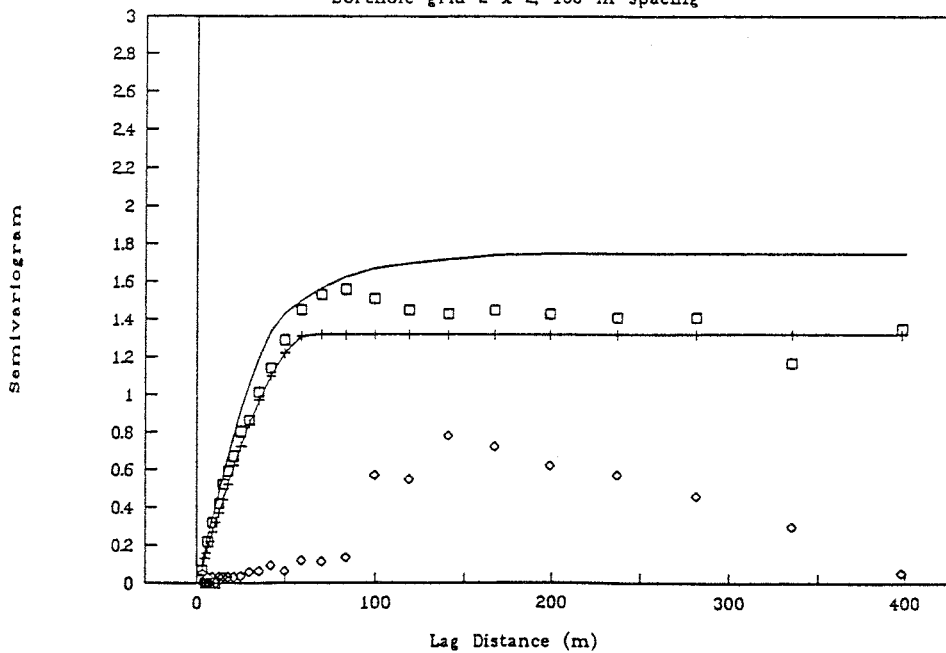
Borehole grid 2 x 2, 100 m spacing



□ Simulated variogram + Fitted model ◊ Weights — Input model

Case Name: testcase\_3s

Borehole grid 2 x 2, 100 m spacing



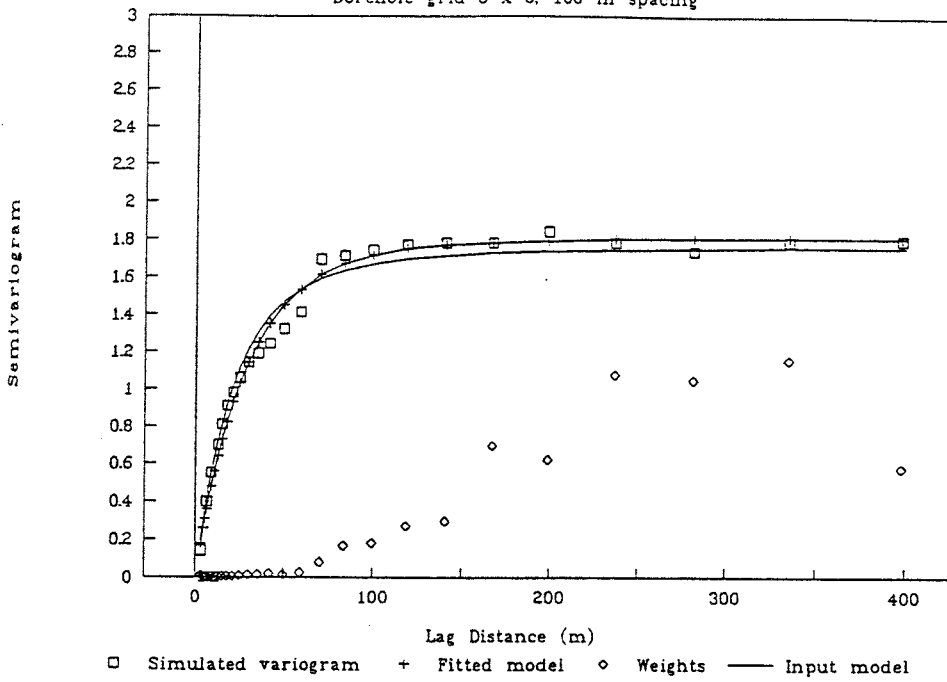
□ Simulated variogram + Fitted model ◊ Weights — Input model

FIGURE 3-6a  
INPUT, FITTED, AND SAMPLE  
VARIogram FOR TESTCASE 3e  
USING 2x2 BOREHOLE GRID

FIGURE 3-6b  
INPUT, FITTED, AND SAMPLE  
VARIogram FOR TESTCASE 3s  
USING 2x2 BOREHOLE GRID

Case Name: testcase\_3e

Borehole grid 5 x 5, 100 m spacing



Case Name: testcase\_3s

Borehole grid 5 x 5, 100 m spacing

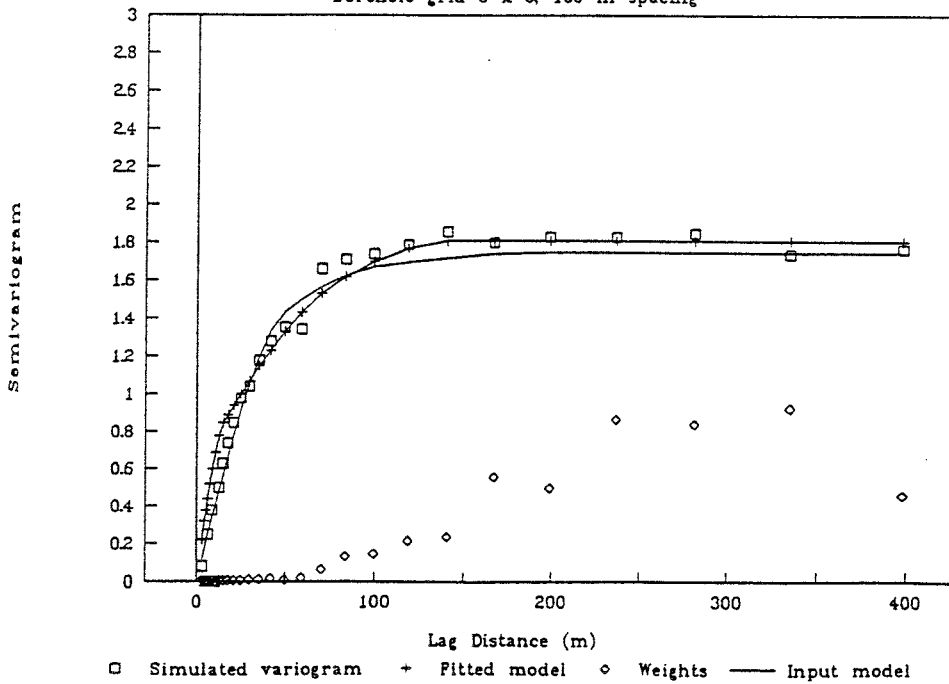


FIGURE 3-7a  
INPUT, FITTED, AND SAMPLE  
VARIOGRAMS FOR TESTCASE 3e  
USING 5x5 BOREHOLE GRID

FIGURE 3-7b  
INPUT, FITTED, AND SAMPLE  
VARIOGRAMS FOR TESTCASE 3s  
USING 5x5 BOREHOLE GRID

An interesting point is that the match of  $\Gamma$  to  $\gamma$  is best at the shorter lags, which have lower weights (*i.e.* fewer number of observations). For the longer lags, despite the large number of observations, the simulated  $\Gamma$  has large discrepancies in relation to  $\gamma$ . This probably is because the observations at long lags are highly interdependent, because of the clustering of measurements along the boreholes, and the correlation of those measurements on a small scale. An improved weighting scheme, taking into account the interdependence of the observations over long lags due to the correlation, is desirable.

### 3.1.4 Test case 4. Nested anisotropic models

The main purpose of Test Case 4 is see whether nested anisotropic models can be resolved by the fitting algorithms, for a given level of contrast and sampling density. Test Case 4 is formed as the summation of 3 horizontally isotropic submodels, with contrasting range and sill values, and mildly contrasting degrees of anisotropy. The following input parameters (with range and anisotropy converted to standardized form) were used for generating synthetic datasets:

Submodel 1	Range = 342 m		
	Sill = 0.25		
	G =	0.117	0
		0	0.117
		0	0
			2.924
Submodel 2	Range = 155 m		
	Sill = 0.5		
	G =	0.194	0
		0	0.194
		0	0
			1.939
Submodel 3	Range = 57 m		
	Sill = 1.5		
	G =	0.617	0
		0	0.617
		0	0
			1.235

The case of exponential submodels was tested. The synthetic regularized data were generated for 3 m measurement spacings, on a 2 x 2 grid of 500 m long, vertical boreholes, with 100 m spacing between holes in the X and Y directions. The following results were obtained:

Exponential covariance: testcase\_4e (SAM 92-865-015)

Submodel 1	Range = 230.2 m		
	Sill = 1.998		
	G =	119	0
		0	119
		0	0
			0.00007
Submodel 2	Range = 35446 m		
	Sill = 0.157		
	G =	0.003	0
		0	0.003
		0	0
			99512
Submodel 3	Range = 46.0 m		
	Sill = 0.005		
	G =	1.28	0
		0	1.28
		0	0
			0.61

The fitted model  $\hat{\gamma}$  is nonsensical, and bears no resemblance to  $\gamma$ , probably because of the small data support relative to the complexity of the model. The huge range in the second submodel

caused INFERENS to stop and give an error message during cross-validation, because the range was more than an order of magnitude larger than the specified width for the kriging neighbourhoods.

A more reasonable model found by the grid-based search, which gave a very slightly worse fit in terms of SSR, was in effect a 2-level nested model:

Submodel 1	Range = 47 m		
	Sill = 1.49		
	G =	1.689	0
		0	1.689
		0	0
			0.351
Submodel 2	Range = 99 m		
	Sill = 0.01		
	G =	1	0
		0	1
		0	0
			1
Submodel 3	Range = 16.0 m		
	Sill = 1.38		
	G =	1.006	0
		0	1.006
		0	0
			0.988

The first fitted submodel resembles the dominant submodel in the input. The other significant submodel, however, bears no relation to the input model. The most likely reason is the small size of the data support.

This test case was repeated for a 5 x 5 grid of vertical boreholes, with the same spacing between holes as before. As described previously, the fitting was performed with respect to lag-class estimates of the semivariogram to make the run time feasible. The model thus estimated was:

Exponential covariance: testcase 4e (SAM 92-865-043)

Submodel 1	Range = 130.3 m		
	Sill = 0.390		
	G =	0.0003	0
		0	0.0003
		0	0
			1.21x10 <sup>8</sup>
Submodel 2	Range = 80.0 m		
	Sill = 0.258		
	G =	0.332	0
		0	0.332
		0	0
			9.10
Submodel 3	Range = 20.1 m		
	Sill = 0.373		
	G =	0.338	0
		0	0.338
		0	0
			8.75



With the larger data support, the fitted model begins to look more reasonable but is still far from the input model. The first fitted submodel has an excessively high degree of anisotropy. The other submodels have approximately the correct degree of anisotropy. The sum of the sill values for the fitted model is, however, just 1.02, whereas the total sill for the input model is 2.25. Thus this fitted model is far off in terms of representing the variance of the input model. Figure 3-8 shows a comparison of  $\hat{\gamma}$  and  $\Gamma$ , illustrating this lack of agreement.

In summary the results of the fitting for a 3-level nested model with horizontal anisotropy are not satisfactory. The problem is probably not due to a bug in the fitting algorithm for horizontally isotropic models, since these were handled reasonably well in Test Case 2. The problem is also probably not due to a bug in the handling of nested models, since Test Case 3 produced  $\hat{\gamma}$  which, though not identical to the input  $\gamma$ , were representative of the simulation  $\Gamma$ . Therefore the problem is believed to be algorithmic (*e.g.* false convergence of the nonlinear regression).

Further investigation of this case is needed. However, the case of nested, horizontally isotropic models may be excessively complicated in relation to its practical interest. This work has been deferred in order to proceed with other verification cases.

### 3.1.5 Test case 5. Nested anisotropic models with different alignment of anisotropy

Test Case 5 is designed to represent the situation of three mutually orthogonal sets of fracture zones (in this case, conveniently aligned perpendicular to each of the coordinate axes). The main purpose is to see if the distinct nested levels can be resolved by the fitting algorithms, for a given level of contrast and sampling density.

The following input parameters (with range and anisotropy converted to standardized form) were used for generating synthetic datasets:

Submodel 1	Range = 342 m			
	Sill = 0.5			
	G =	0.117	0	0
		0	0.117	0
		0	0	2.924
Submodel 2	Range = 86 m			
	Sill = 0.5			
	G =	0.464	0	0
		0	4.64	0
		0	0	0.464
Submodel 3	Range = 65 m			
	Sill = 1.0			
	G =	4.64	0	0
		0	0.464	0
		0	0	0.464

The case of exponential submodels was tested. The synthetic regularized data were generated for 3 m measurement spacings, on a 2 x 2 grid of 500 m long, vertical boreholes, with 100 m spacing between holes in the X and Y directions. The following results were obtained:

Exponential covariance: testcase\_5e (SAM 92-865-016)

Submodel 1	Range = 115.2 m			
	Sill = 1.01			
	G =	1.29	0	0
		0	1.29	0
		0	0	0.596
Submodel 2	Range = 23.8 m			
	Sill = 0.64			
	G =	0.024	0	0
		0	166.	0
		0	0	0.254
Submodel 3	Range = 263.1 m			
	Sill = 0.01			
	G =	0.55	0	0
		0	0.34	0
		0	0	5.3

Cross-validation statistics:

$$\begin{aligned} \text{MRE} &= 0.000386 \\ \text{MSRE}^{1/2} &= 1.04 \\ \text{MSE}^{1/2} &= 0.419 \end{aligned}$$

The third submodel is negligible due to the near-zero variance, so in effect the fitted model is a two-level nested model, consisting of an approximately isotropic model with slightly extended range in the Z direction, and a second component with strong anisotropy giving enhanced correlation in the X direction and, to a lesser extent, the Z direction.

Thus the nested fitting algorithm has succeeded in distinguishing the main anisotropy of the input model (the strong correlation in the Y direction, in Submodel 3, is partly cancelled by the reduced Y-direction range in Submodel 2). However, the resolution possible for this level of data support seems to be rather limited.

Due to the rather complicated model, it is difficult to construct plots to compare  $\gamma$ ,  $\Gamma$ , and  $\hat{\gamma}$ . However, the cross-validation statistics for this model are very good, indicating that the fitted model is an excellent kriging predictor of the simulated data set. Thus, despite the dissimilarity between the input model and the fitted model, on a component-by-component basis, INFERENS appears to have succeeded in converging to a fitted  $\hat{\gamma}$  which is a good approximation to  $\Gamma$ .

This test case was also repeated for a 5 x 5 grid of vertical boreholes, with the same spacing between holes as before. As described previously, the fitting was performed with respect to lag-class estimates of the semivariogram to make the run time feasible. The model thus estimated was (SAM 92-865-044):

Submodel 1	Range = 300.2 m		
	Sill = 2.32		
	G =	0.927	0
		0	0.927
		0	0
			1.16
Submodel 2	Range = 444 m		
	Sill = 0.01		
	G =	1.08	0
		0	8.48
		0	0
			0.109
Submodel 3	Range = 445 m		
	Sill = 0.01		
	G =	1.01	0
		0	0.48
		0	0
			2.06

The last two submodels are negligible, and so the resulting model is essentially a simple, isotropic model with a range of 300 m. The cross-validation check failed (because of a memory allocation error -- apparently the dimension of RDYN needed to be increased, as for Case 3).

### 3.2 Simultaneous estimation of covariance models and trend functions

The test cases described above were extended to test IGLSE fitting of trend functions and covariance models. The IGLSE test cases were constructed by adding three known trend functions to each of the test cases described in the previous section:

$$\begin{array}{ll}
 \text{Constant trend function:} & \beta_1 = -6.0 \\
 \text{Logarithmic trend function:} & \beta_2 = 2.0 \quad (\text{Constant } A = 40) \\
 \text{Zone trend function:} & \beta_3 = 1.0 \quad (\text{Horizontal zone from 175 to 275 m depth})
 \end{array}$$

The simulation of the trend functions was checked visually by plotting the simulated data as a function of depth, and by plotting the residuals (after subtracting the known trend) versus depth.

Preliminary attempts at fitting trend functions, during debugging, included trend functions in combination with the more complicated test cases (4 and 5) described in the previous section. However, due to the difficulties experienced in fitting the intrinsic versions of the nested model test cases, in the final runs no attempt was made to fit trend functions with test cases 4 and 5.

The results are given below. The input model for each IGLSE test case (*e.g.* testcase\_1etf) is identical to the corresponding intrinsic case (*e.g.* testcase\_1e), except for the addition of the trends.

The data support for the IGLSE test cases was a 3 x 3 grid of 500 m deep boreholes, with 100 m spacing in the X and Y directions.

The estimated 95% confidence ellipsoids for the  $\beta_i$  were unbelievably huge in all cases. The mathematics and code for calculating the confidence ellipsoids needs to be checked. However, since this calculation is performed at the end of the fitting, it does not affect the quality of the results given here.

Exponential covariance: testcase\_1etf (SAM 92-865-020)

Fitted model:

$$\begin{aligned}\beta_1 &= -5.364 \\ \beta_2 &= 2.215 \\ \beta_3 &= 1.233 \\ \text{Range} &= 63.209 \\ \text{Sill} &= 1.5748\end{aligned}$$

Cross-validation statistics:

$$\begin{aligned}\text{MRE} &= -0.0165 \\ \text{MSRE}^{1/2} &= 0.866 \\ \text{MSE}^{1/2} &= 0.41\end{aligned}$$

Spherical covariance: testcase\_1stf (SAM 92-865-021)

Fitted model:

$$\begin{aligned}\beta_1 &= -7.362 \\ \beta_2 &= 1.49 \\ \beta_3 &= 0.8877 \\ \text{Range} &= 75.969 \\ \text{Sill} &= 1.6439\end{aligned}$$

Cross-validation statistics:

$$\begin{aligned}\text{MRE} &= -0.00388 \\ \text{MSRE}^{1/2} &= 0.943 \\ \text{MSE}^{1/2} &= 0.297\end{aligned}$$

Figure 3-9a,b show the input and fitted trends for the two cases. The fitted covariance and trend models are in both cases reasonably close to the input models. For this model there is some redundancy in the model:

$$\log K = \beta_1 - \beta_2 \log(A+z) + \beta_3 I(x,y,z) \quad (3-5)$$

which can be seen if this is written in the form:

$$\log K = \beta_1 - \beta_2 f(z) + \beta_3 I(x,y,z), \quad 1.6 < f(z) < 2.73 \quad (3-6)$$

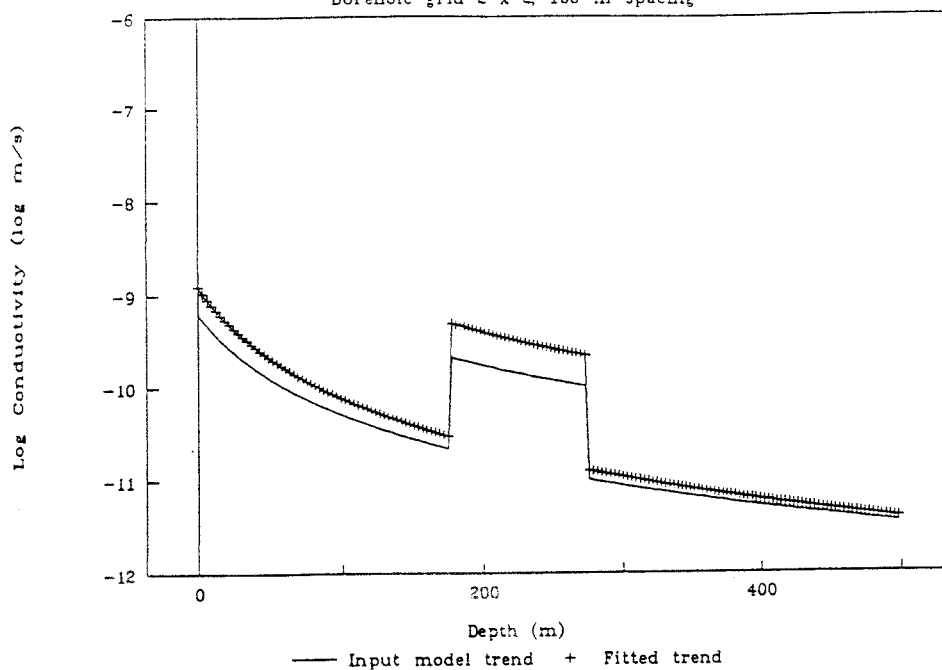
for the tested case of 500 m deep boreholes and  $A = 40$ , or:

$$\log K = (\beta_1 - 1.6\beta_2) + \beta_2(f(z) - 1.6) + \beta_3 I(x,y,z) \quad (3-7)$$

Therefore it is appropriate to compare estimates of  $(\beta_1 - 1.6 \beta_2)$  and  $\beta_2$  with the input values. On this basis, it is seen that the term  $(\beta_1 - 1.6 \beta_2)$  is estimated within about  $\pm 6\%$ , and  $\beta_2$  and  $\beta_2$  both within  $\pm 25\%$ . In the exponential case both  $\beta_2$  and  $\beta_3$  have been slightly overestimated, while in the spherical case both have been slightly underestimated. However, as seen in the figures, the composite trend is within 0.25 log m/s, *i.e.* within about 20 percent of the standard deviation of the random component.

Case Name: testcase\_1etf

Borehole grid 2 x 2, 100 m spacing



Case Name: testcase\_1stf

Borehole grid 2 x 2, 100 m spacing

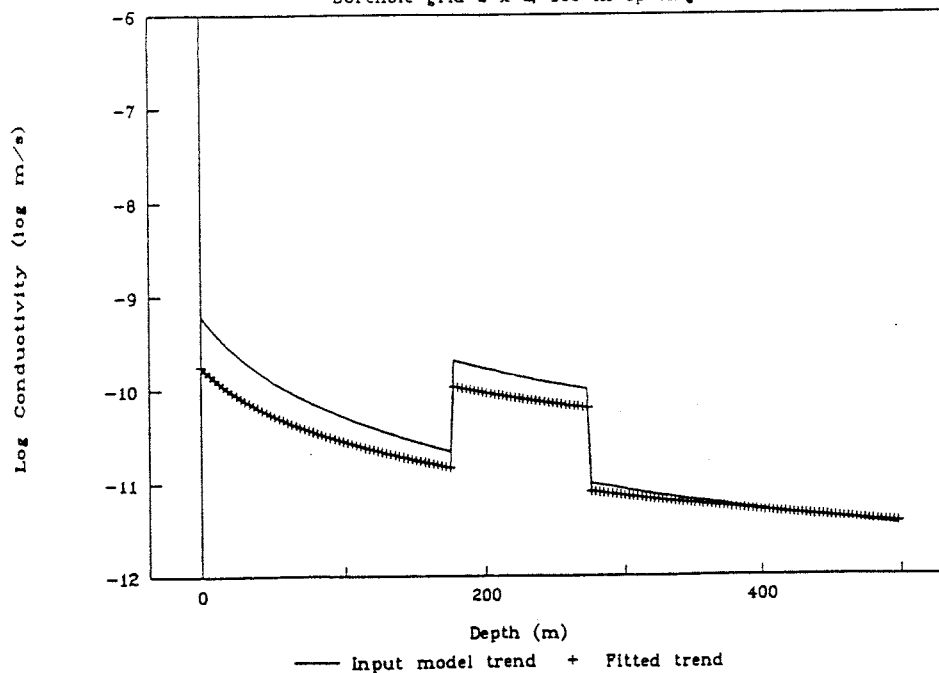


FIGURE 3-8a

INPUT AND FITTED TRENDS FOR SIMPLE ISOTROPIC COVARIANCE (test case\_1etf) WITH POTENTIAL-TYPE TRENDS

FIGURE 3-8b

INPUT AND FITTED TRENDS FOR SIMPLE ISOTROPIC COVARIANCE (test case\_1stf) WITH POTENTIAL-TYPE TRENDS

Exponential covariance: testcase\_2etf (SAM 92-865-022)

Fitted model:

$$\begin{aligned}
 \beta_1 &= -14.73 \\
 \beta_2 &= -1.312 \\
 \beta_3 &= 1.185 \\
 \text{Range} &= 107.24 \\
 \text{Sill} &= 1.3256 \\
 \mathbf{G} &= \begin{matrix} 0.777 & 0 & 0 \\ 0 & 0.777 & 0 \\ 0 & 0 & 1.66 \end{matrix}
 \end{aligned}$$

Cross-validation statistics:

$$\begin{aligned}
 \text{MRE} &= 0.00903 \\
 \text{MSRE}^{1/2} &= 1.02 \\
 \text{MSE}^{1/2} &= 0.438
 \end{aligned}$$

Spherical covariance: testcase\_2stf (SAM 92-865-023)

$$\begin{aligned}
 \beta_1 &= -5.068 \\
 \beta_2 &= 2.352 \\
 \beta_3 &= 0.8592 \\
 \text{Range} &= 93.733 \\
 \text{Sill} &= 1.3508 \\
 \mathbf{G} &= \begin{matrix} 0.653 & 0 & 0 \\ 0 & 0.653 & 0 \\ 0 & 0 & 2.35 \end{matrix}
 \end{aligned}$$

Cross-validation statistics:

$$\begin{aligned}
 \text{MRE} &= -0.00259 \\
 \text{MSRE}^{1/2} &= 1.09 \\
 \text{MSE}^{1/2} &= 0.43
 \end{aligned}$$

In both cases the covariance models, including anisotropy, seem to be properly estimated, in view of the level of data support. In the spherical case, the grid-based search found two distinct local minima; the parameter estimates for the better fit are the ones reported above.

The input and fitted trends are shown in Figure 3-10a,b.

In the exponential case, all searches converged to the same optimum, with  $(\beta_1, \beta_2)$  and  $\beta_3$  far from the input values, while  $\beta_3$ , representing the zone effect, was estimated close to the input value. The composite fitted trend is far from the input model at shallow depths, as shown in Figure 3-10a, although at depth the composite input and fitted trends are close to each other.

The spherical case, on the other hand, yielded a very good match as is evident from Figure 3-10b.

Despite the obvious disagreement for the exponential case, the cross-validation statistics are excellent, indicating that the fitted model yields a good kriging predictor of the simulated dataset.



This result should be seen as a caution against placing too much trust in the cross-validation statistics, as an indicator of the goodness of the overall model including trend parameters.

Possibly the misleadingly good statistics are produced because the cross-validation employed horizontal kriging neighborhoods, which could take care of the error in trend estimation. A more stringent test of a model with trend functions might be to use global kriging (or equivalently, to make the kriging neighborhoods sufficiently large that all points are contained in a single neighborhood) of the residuals after removing the estimated trend.

However, even global kriging, in connection with the "delete-one" cross-validation procedure, may not provide a sufficiently stringent test, since the kriged estimate at each deleted datapoint will be strongly dependent on the nearest points in the same borehole, which have nearly the same value of the trend. Cross-validation by deleting larger sections of the dataset (e.g. a complete borehole) would probably provide a better test of residual models.

The bad results in the exponential case indicate that even with a grid-based search for covariance model parameters, there is a chance for INFERENS to get stuck at an incorrect local minimum for the trend parameters. In INFERENS 1.1, the starting estimate for the parameter vector  $\beta$ , for each IGLSE search, is obtained by ordinary least squares regression, as described in Section 2.3. As a result the starting estimate of  $\beta$  is always the same for a given dataset, independent of the value of the covariance model parameter vector  $\mathbf{p}$  specified by the grid-based search algorithm.

The first step in the IGLSE process is thus always to search for the optimum  $\mathbf{p}$  for the OLSR estimate of  $\beta$ , starting from the grid-specified value of  $\mathbf{p}$ . If this step always yields the same estimate of  $\mathbf{p}$ , the fitted models will be identical for all starting points in the grid. As the results for the exponential case illustrate, when this happens the fitted model may not necessarily be the correct one.

One possible improvement would be to introduce variable starting points  $\beta$ , by using a random or deterministic perturbation of the OLSR estimate of  $\beta$ . It would probably be better to have INFERENS do this automatically, rather than having the analyst supply a list of values (as is done for the grid-based search in  $\mathbf{p}$ ), since the analyst is not likely to have any more sensible estimate of  $\beta$ , *a priori*, than is given by the OLSR estimate.

Better yet, the fitting process could be converted from IGLSE to an ordinary, nonlinear least-squares regression problem, treating the combined parameter vector  $\mathbf{P} = [\beta, \mathbf{p}]$ . This would allow fitting of trend function parameters which lead to non-linear estimation problems (as discussed by Norman, 1992a). The code development for this consists mainly of eliminating the IGLSE routines, so the resulting code would be simpler. Some new routines would be required to calculate derivatives of the sum of residuals squared, with respect to the trend function parameters.

**Exponential covariance: testcase\_3etf**

Fitted model (SAM 92-865-024; run was aborted after 3 IGLSE steps):

$$\begin{aligned}\beta_1 &= -4.334 \\ \beta_2 &= 2.664 \\ \beta_3 &= 1.327\end{aligned}$$

Submodel 1	Range = 54.4 m
	Sill = 0.815
Submodel 2	Range = 57.2 m
	Sill = 1.008
Submodel 3	Range = 51.8 m
	Sill = 0.4842

This test run was terminated early because it seemed to be converging toward results similar to testcase\_3e, with a lack of distinction between nested submodels.

#### 4. PRELIMINARY APPLICATION TO THE FINNSJÖN DATASET

To demonstrate INFERENS 1.1, the code was applied to a dataset from Finnsjön which was previously analyzed by Norman (1992a), using INFERENS 1.0. The data consisted of hydraulic conductivity estimates from constant-head packer tests in the boreholes HFI01, BFI01-02, and KFI01-11. The data were obtained from the GEOTAB database as described by Norman (1992a). The test section lengths represented in the raw data included 2 m, 3 m, 5 m, and 10 m intervals. The conductivity values as found in GEOTAB were from steady-state interpretations of the constant-head tests, using the formula of Moye (1967).

These data were regularized using INFERENS prior to fitting each model. A regularization scale of 36 m was used in all cases. The kriging neighborhoods, kriging sets, and regularization tolerances used in these runs were identical to those used by Norman. For the lag-class estimation cases, only 40 radial lag classes were used (compared with 91 used by Norman) and, in the case of anisotropic models, more angular lag classes were used (depending on the type of anisotropic model being treated). The weighting of the lag class estimates was proportional to the number of data pairs in each lag class. A slightly simplified representation of Zone 2, based on the two bounding planes fitted by regression in Appendix E of Norman. The demonstration runs were limited to the case of regularization on a 36 m scale, which was the case presented in detail by Norman.

Certain of the cases are thus directly comparable to those considered by Norman, except for the minor differences in lag classes and Zone 2 definition. The other cases, however, are significantly different from those considered by Norman, either because direct fitting to the data (without lag classes) was used, or because new types of models supported by INFERENS 1.1 were used.

The following sections present the results which were obtained for various types of covariance models and fitting methods, for both intrinsic models and potential-type trend models.

For exponential models, the range values reported are the *practical range* equal to  $3/\lambda$ . In the case of isotropic models, the analyses are omni-directional rather than in a specific direction.

## 4.1 Intrinsic models

### 4.1.1 Isotropic models

#### Case fiiein36: Isotropic exponential model (direct fitting) (SAM 92-865-029)

Range = 417.45

Sill = 2.0139

Cross-validation statistics:

MRE = 0.00499

MSRE<sup>1/2</sup> = 1.06

MSE<sup>1/2</sup> = 0.193

#### Case fiieil36: Isotropic exponential model (lag-class fitting) (SAM 92-865-030)

Range = 499.86

Sill = 1.9705

Cross-validation statistics:

MRE = 0.0048

MSRE<sup>1/2</sup> = 1.17

MSE<sup>1/2</sup> = 0.193

#### Case fiisin36: Isotropic spherical model (direct fitting) (SAM 92-865-031)

Range = 389.65

Sill = 1.7636

Cross-validation statistics:

MRE = 0.00459

MSRE<sup>1/2</sup> = 1.54

MSE<sup>1/2</sup> = 0.193

#### Case fiisil36: Isotropic spherical model (lag-class fitting) (SAM 92-865-032)

Range = 405.79

Sill = 1.9027

Cross-validation statistics:

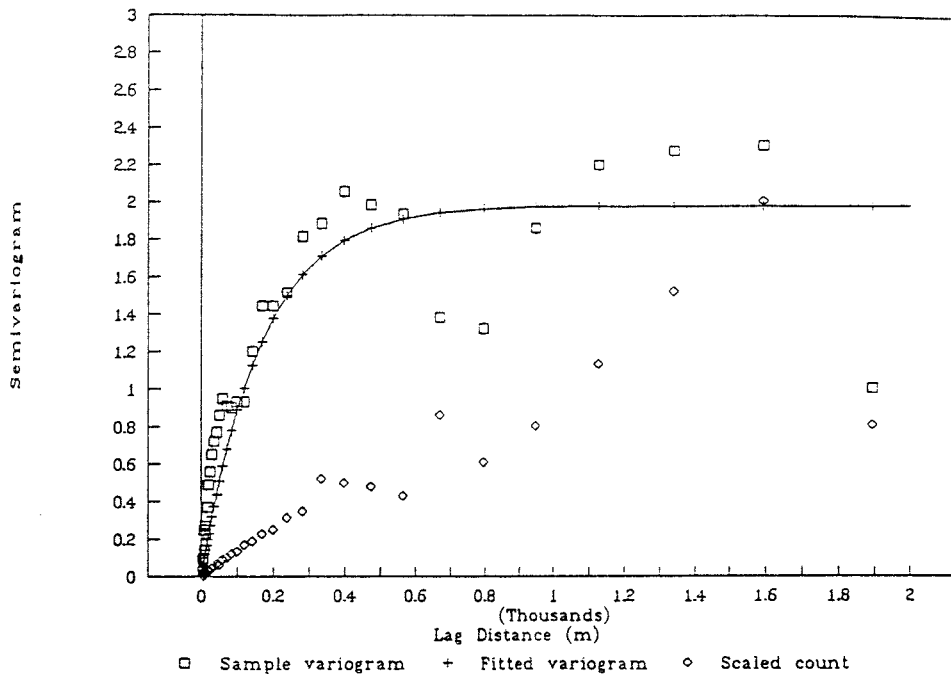
MRE = 0.00466

MSRE<sup>1/2</sup> = 1.52

MSE<sup>1/2</sup> = 0.193

In both spherical and exponential cases the models obtained with and without lag classes are quite similar, and there is little difference in terms of the cross-validation statistics. In comparison with the results of Norman (1992a), these models have larger ranges (by a factor of 1.3 to 1.4) and slightly higher variance (by a factor of 1.1 to 1.15), than the results previously obtained by Norman (1992a). Presumably the differences are due mainly to the sensitivity to choice of lag classes, which was demonstrated by Norman. The cross-validation statistics are somewhat worse with the newer fits, suggesting that the particular lag-class division and weighting scheme used by Norman was more appropriate for estimating the best model for prediction using kriging.

Case: fiieil36



Case: fiiein36

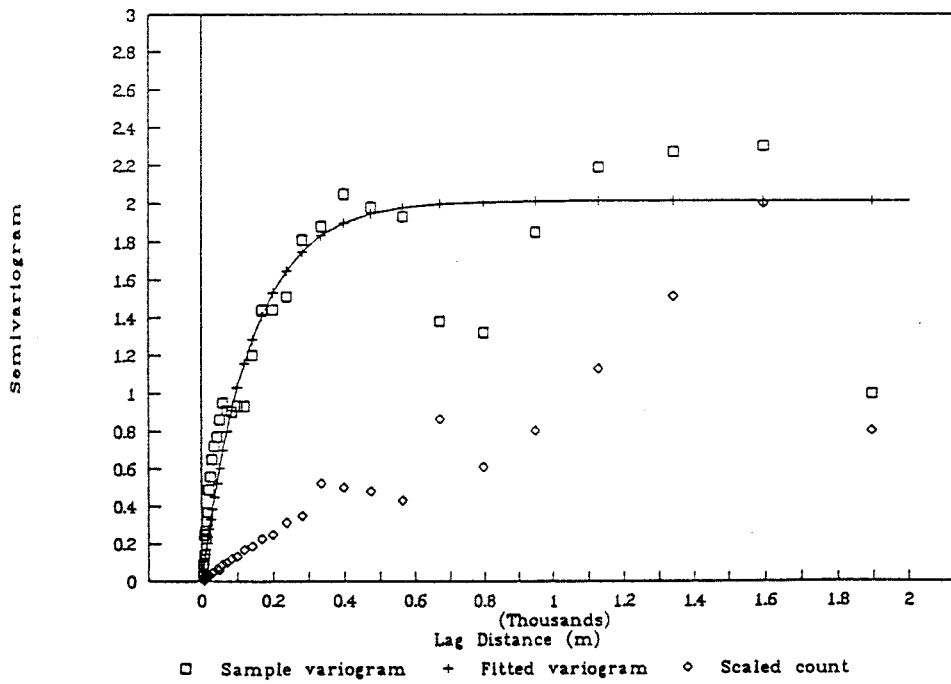
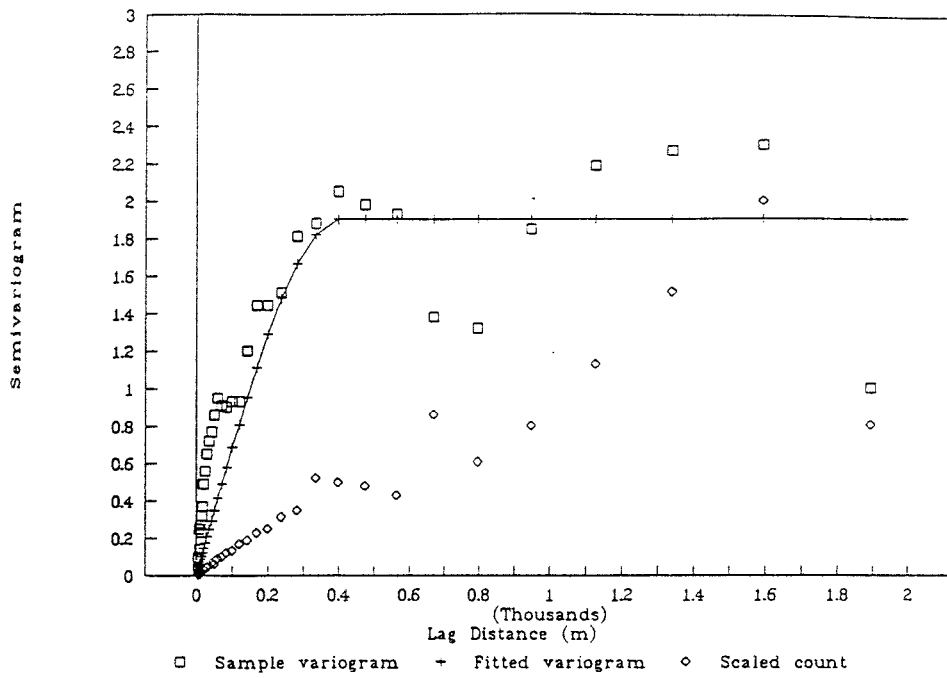


FIGURE 4-1ab  
FINNSJÖN DATA INTRINSIC  
EXPONENTIAL ISOTROPIC  
MODEL (lag classes, direct).

Case: fiisil36



Case: fiisin36

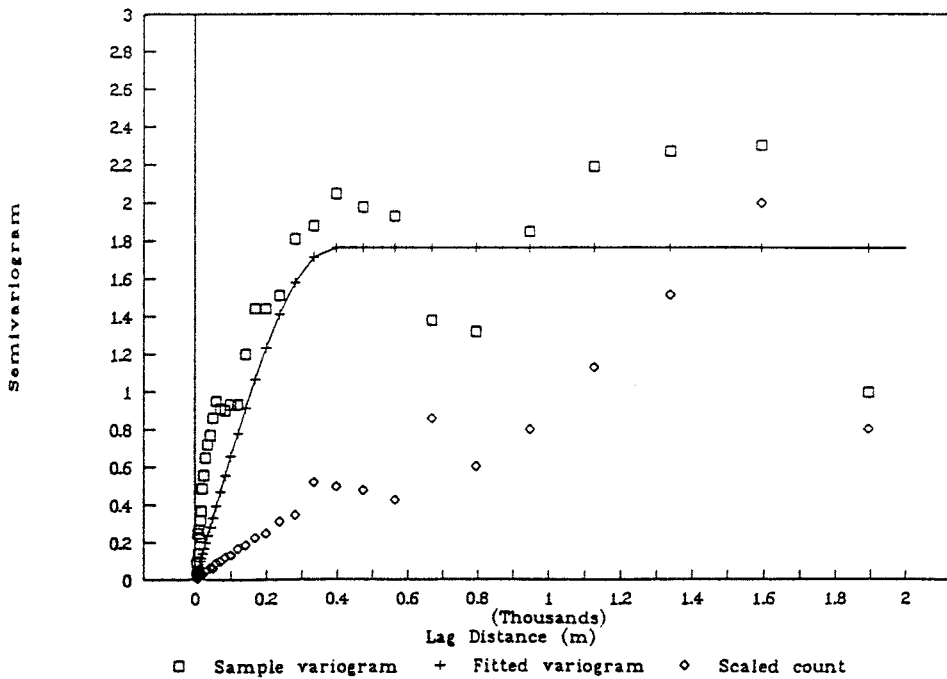


FIGURE 4-2ab  
FINNSJÖN DATA INTRINSIC  
SPHERICAL ISOTROPIC  
MODEL (lag classes, direct).

#### 4.1.2 Horizontally isotropic models

##### Case fiiehn36: Horizontally isotropic exponential model (direct fitting) (SAM 92-865-025)

Range = 625.2  
 Sill = 2.49  
 G =  $\begin{matrix} 0.583 & 0 & 0 \\ 0 & 0.583 & 0 \\ 0 & 0 & 2.94 \end{matrix}$

##### Directional ranges:

Horizontal range = 1072 m  
 Vertical range = 212 m

##### Cross-validation statistics:

MRE = 0.00605  
 MSRE<sup>1/2</sup> = 0.710  
 MSE<sup>1/2</sup> = 0.196

##### Case fiiehl36: Horizontally isotropic exponential model (lag-class fitting) (SAM 92-865-026)

Range = 300.1  
 Sill = 1.90  
 G =  $\begin{matrix} 0.975 & 0 & 0 \\ 0 & 0.975 & 0 \\ 0 & 0 & 1.05 \end{matrix}$

##### Directional ranges:

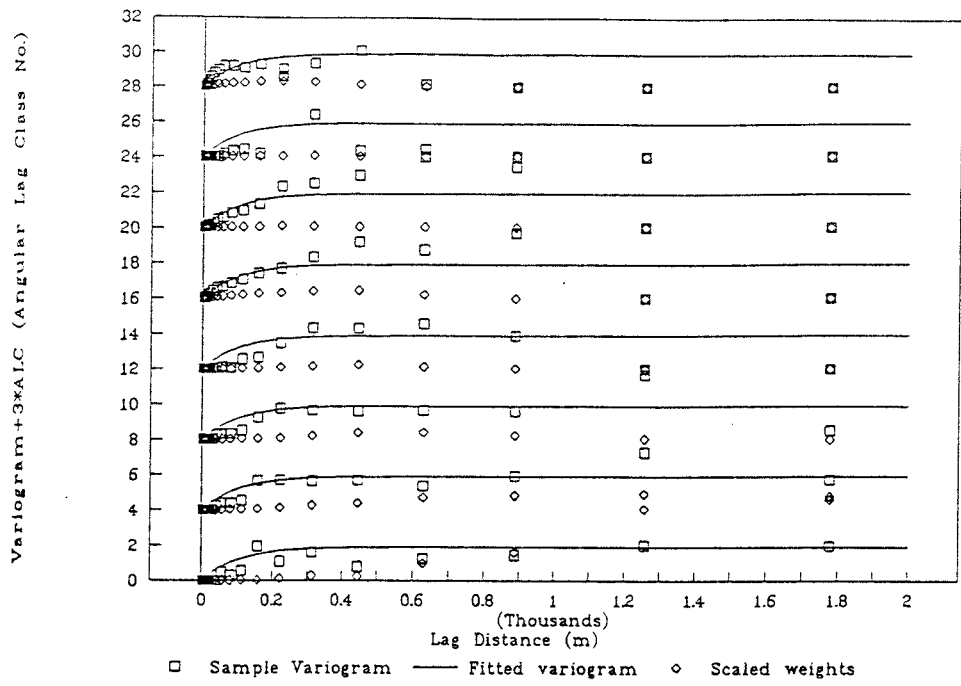
Horizontal range = 308 m  
 Vertical range = 286 m

##### Cross-validation statistics:

MRE = 0.00524  
 MSRE<sup>1/2</sup> = 0.906  
 MSE<sup>1/2</sup> = 0.194

Figure 4-3 presents fitted and sample semivariograms for the cases of lag-class and direct fitting.

Case: fiiehl36



Case: fiiehn36

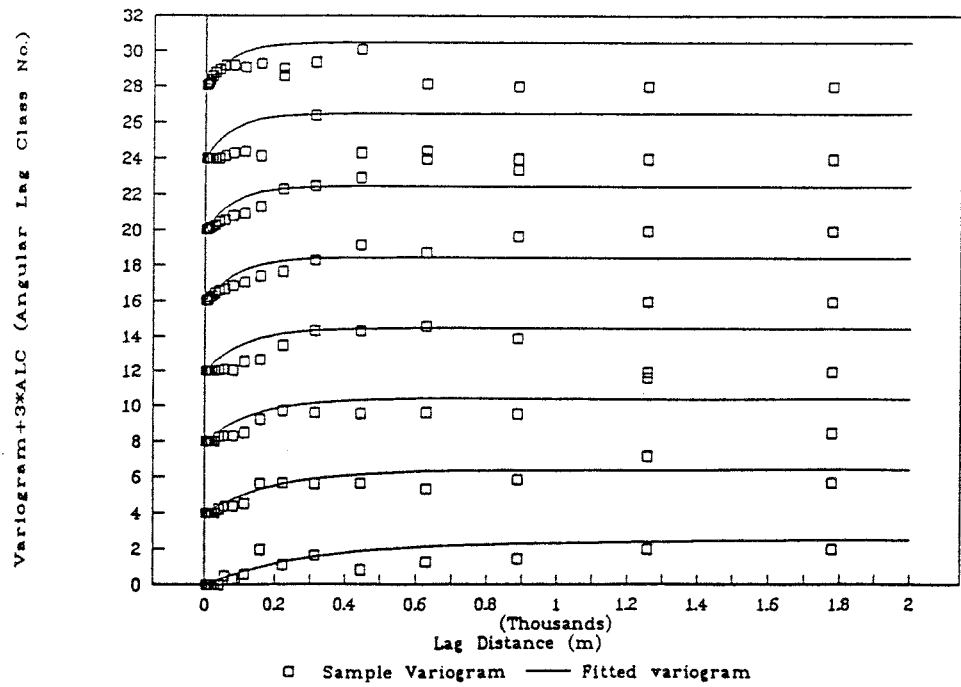


FIGURE 4-3ab  
FINNSJÖN DATA INTRINSIC  
EXPONENTIAL HORIZONTALLY  
ISOTROPIC MODEL (lag classes,  
direct).



Case fiishn36: Horizontally isotropic spherical model (direct fitting) (SAM 92-865-028)

Range = 751.8  
 Sill = 1.79  
 G =   0.514   0       0  
       0       0.514   0  
       0       0       3.79

## Directional ranges:

Horizontal range = 1463 m  
 Vertical range = 198 m

## Cross-validation statistics:

MRE = 0.00506  
 MSRE<sup>1/2</sup> = 1.14  
 MSE<sup>1/2</sup> = 0.194

Case fiishl36: Horizontally isotropic spherical model (lag-class fitting) (SAM 92-865-027)

Range = 300.03  
 Sill = 1.9052  
 G =   0.975   0       0  
       0       0.975   0  
       0       0       1.05

## Directional ranges:

Horizontal range = 308 m  
 Vertical range = 286 m

## Cross-validation statistics:

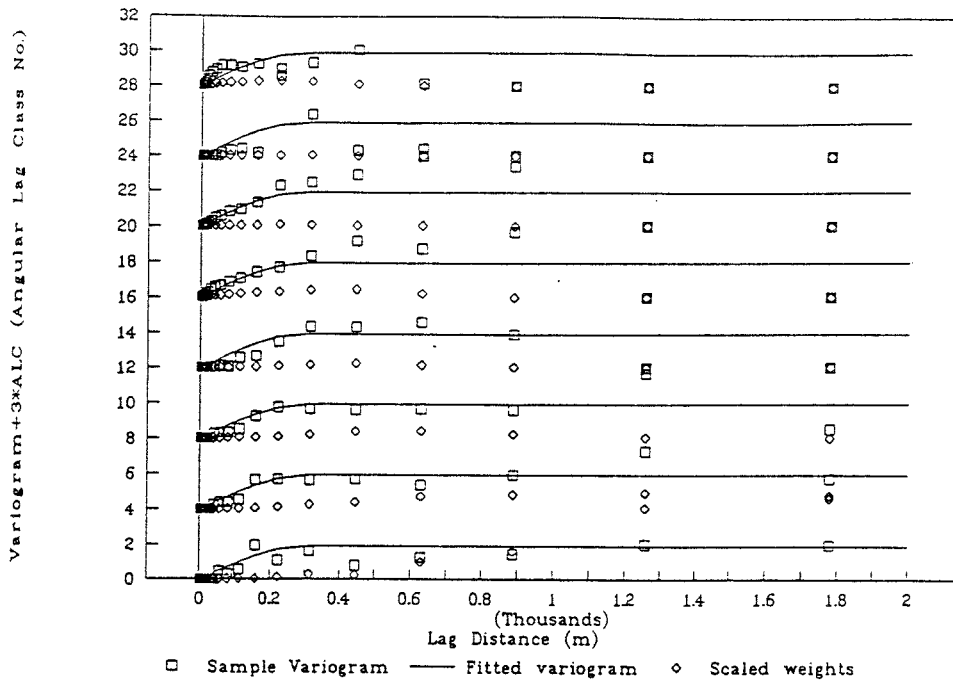
MRE = 0.00493  
 MSRE<sup>1/2</sup> = 1.28  
 MSE<sup>1/2</sup> = 0.193

Comparison of the lag-class and direct estimates, in both exponential and spherical cases, shows a strong sensitivity of the results to lag class definition. The direct fitting give much higher anisotropy than the lag-class fitting, for the particular choice of lag classes used. In terms of MRE and MSRE, the best model appears to be the spherical model fitted directly to the data, which is better than the corresponding isotropic model.

Curiously the directly-fitted, horizontally isotropic, exponential model is much worse than the corresponding isotropic model, in terms of MRE and MSRE. This observation is consistent with the results presented by Norman (1992a).

The estimated degree of anisotropy for the directly-fitted models is similar to that estimated by Norman (1992a) for the exponential case.

Case: fiishl36



Case: fiishn36

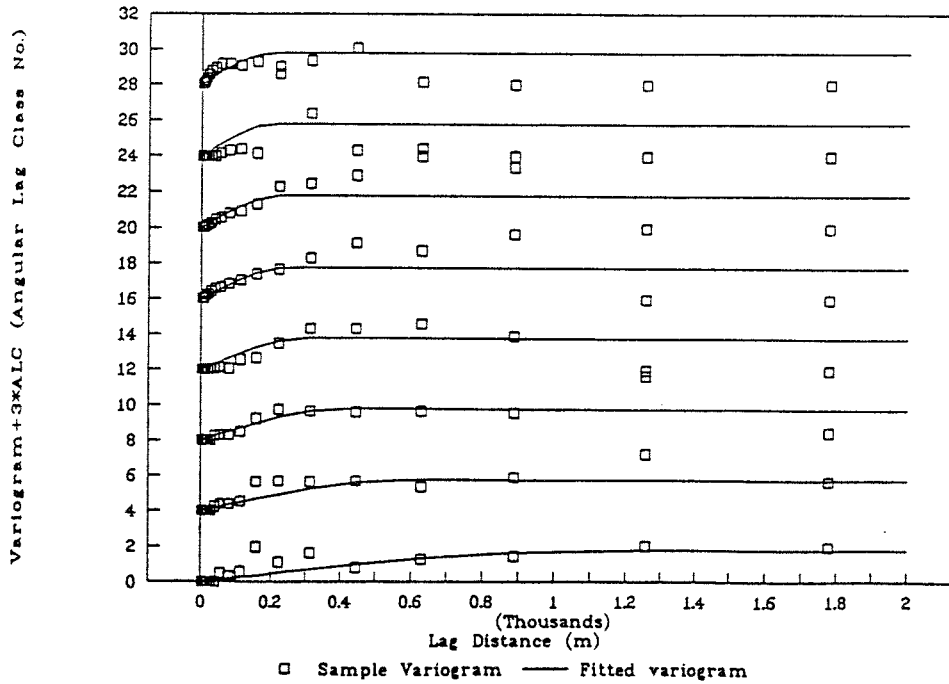


FIGURE 4-4ab  
FINNSJÖN DATA INTRINSIC SPHERICAL  
HORIZONTALLY ISOTROPIC MODEL (lag classes, direct).

### 4.1.3 Nested isotropic models

Case fiienl36: Nested isotropic exponential model (lag-class fitting) (SAM 92-865-033)

Minimum SSR fit from grid-based search:

Submodel 1: Range = 511.4 m  
               Sill = 0.158  
 Submodel 2: Range = 78.3 m  
               Sill = 0.04

Cross-validation statistics:

MRE = 0.00119  
 MSRE<sup>1/2</sup> = 1.61  
 MSE<sup>1/2</sup> = 0.194

In spite of giving the best fit in terms of SSR, this is a poor model as seen from the variances and the cross-validation statistics. The second-best model, from the grid-based search, was much more reasonable:

Submodel 1: Range = 499.2 m  
               Sill = 1.359  
 Submodel 2: Range = 99.2 m  
               Sill = 0.579

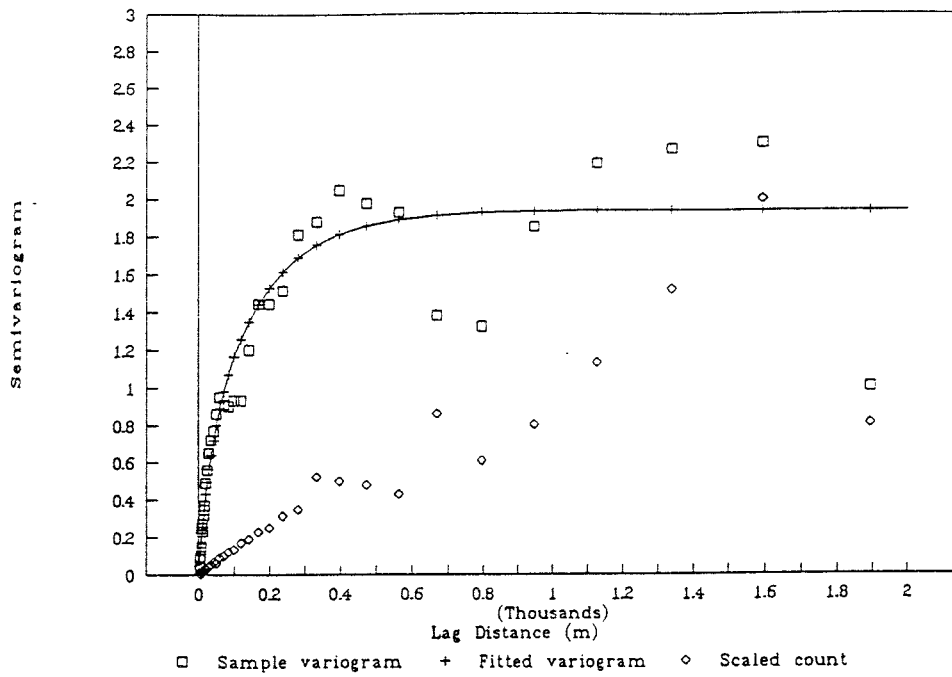
Comparison with the results obtained by Norman (1992a, Section 9.2.2) by restricting the fitting to lags less than 130 m, suggested that this could be a superior model. Figure 4-5a compares this model with the sample semivariogram. In comparison with the simple isotropic models presented above, this model gives a markedly better fit to the sample semivariogram at moderately short (< 100 m) lags. The model also represents the full variance at longer lags, which could not be achieved by fitting a simple isotropic model to just the shorter lags (Norman 1992a).

Cross-validation statistics for this model were obtained by a second run of INFERENS (SAM 92-865-051):

MRE = 0.000555  
 MSRE<sup>1/2</sup> = 0.797  
 MSE<sup>1/2</sup> = 0.194

This is definitely an improvement over the nested model given above, but it is still unacceptable (assuming that the distributions of MSRE<sup>1/2</sup> is similar to that for the simple covariance models).

Case: fiienl36



Case: fiisnl36

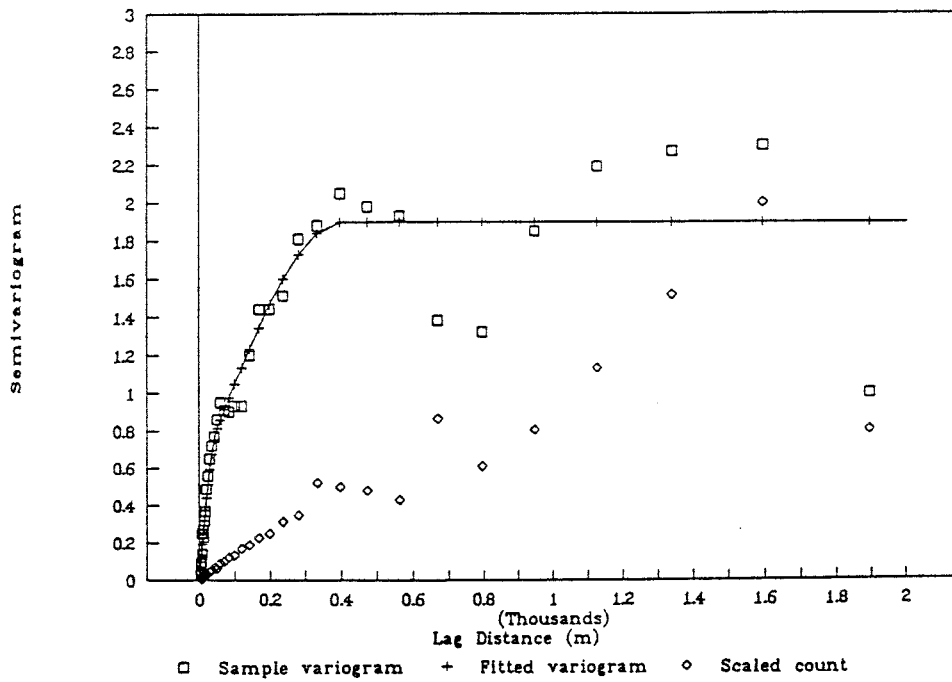


FIGURE 4-5ab  
FINNSJÖN DATA INTRINSIC  
NESTED ISOTROPIC MODELS  
(exponential, spherical).

Case fiisnl36: Nested isotropic spherical model (lag-class fitting) (SAM 92-865-047)

Minimum SSR fit from grid-based search:

Submodel 1: Range = 405.8 m  
Sill = 1.328  
Submodel 2: Range = 49.8 m  
Sill = 0.569

Cross-validation statistics:

MRE = 0.00517  
MSRE<sup>1/2</sup> = 0.858  
MSE<sup>1/2</sup> = 0.194

A comparison of the fitted model with the sample semivariogram (Figure 4-5b) shows that this gives a very close fit up to about 500 m. Visually this seems to be a better model than the nested exponential model, which is able to fit the rather sharp "kinks" in the sample semivariogram around 50 m and 400 m. However, in terms of cross-validation statistics this model is still not very good.

#### 4.1.4 Anisotropic models

The new possibility to fit an anisotropic model, with principal directions of anisotropy aligned with the X,Y, and Z axes, was demonstrated for cases of exponential and spherical covariance, using direct fitting to the data. The estimated models, as given below, are very similar to the corresponding cases with horizontally isotropic models. The estimated degree of statistical anisotropy in the horizontal plane is just 1.3 to 1.5, *i.e.* nearly isotropic.

The cross-validation statistics are only marginally better than the corresponding horizontally isotropic cases.

##### Case fiixn36: Anisotropic exponential model (direct fitting) (SAM 92-865-049)

Range = 632.1  
 Sill = 2.475  
 G =  $\begin{matrix} 0.663 & 0 & 0 \\ 0 & 0.514 & 0 \\ 0 & 0 & 2.93 \end{matrix}$

Directional ranges:

Horizontal (X) range = 953 m  
 Horizontal (Y) range = 1230 m  
 Vertical range = 216 m

Cross-validation statistics:

MRE = 0.00601  
 MSRE<sup>1/2</sup> = 0.717  
 MSE<sup>1/2</sup> = 0.196

##### Case fiisxn36: Anisotropic spherical model (direct fitting) (SAM 92-865-050)

Range = 681.1  
 Sill = 1.892  
 G =  $\begin{matrix} 0.766 & 0 & 0 \\ 0 & 0.480 & 0 \\ 0 & 0 & 2.72 \end{matrix}$

Directional ranges:

Horizontal (X) range = 889 m  
 Horizontal (Y) range = 1419 m  
 Vertical range = 250 m

Cross-validation statistics:

MRE = 0.00490  
 MSRE<sup>1/2</sup> = 1.24  
 MSE<sup>1/2</sup> = 0.193

## 4.2 Models with potential-type trends

Demonstrations were also performed of fitting to a potential-type trend function:

$$\log K = \beta_1 - \beta_2 \log(A+z) + \beta_3 I(x,y,z) \quad (4-1)$$

as used in the trend function verification cases, where in this case  $I(x,y,z) = 1$  only if the point is in Zone 2. This is the same type of composite trend function as was treated in Section 9.3.1 of Norman (1992a). Note however, that the numbering of the parameters is different.

### 4.2.1 Isotropic models

#### Case fipein36: Exponential isotropic model (direct fitting) (SAM 92-865-037)

$$\begin{aligned} \beta_1 &= -2.74 \\ \beta_2 &= 1.648 \\ \beta_3 &= 0.058024 \\ \text{Range} &= 1490.3 \\ \text{Sill} &= 0.67254 \end{aligned}$$

Cross-validation statistics:

$$\begin{aligned} \text{MRE} &= 0.00531 \\ \text{MSRE}^{1/2} &= 3.45 \\ \text{MSE}^{1/2} &= 0.192 \end{aligned}$$

#### Case fipeil36: Exponential isotropic model (lag-class fitting) (SAM 92-865-035)

$$\begin{aligned} \beta_1 &= -2.185 \\ \beta_2 &= 1.978 \\ \beta_3 &= 0.067171 \\ \text{Range} &= 300.58 \\ \text{Sill} &= 1.4872 \end{aligned}$$

Cross-validation statistics:

$$\begin{aligned} \text{MRE} &= 0.00299 \\ \text{MSRE}^{1/2} &= 1.04 \\ \text{MSE}^{1/2} &= 0.193 \end{aligned}$$

#### Case fipsin36: Spherical isotropic model (direct fitting) (SAM 92-865-048)

$$\begin{aligned} \beta_1 &= -3.023 \\ \beta_2 &= 1.564 \\ \beta_3 &= 0.057546 \\ \text{Range} &= 544.9 \\ \text{Sill} &= 0.643 \end{aligned}$$

Cross-validation statistics:

$$\begin{aligned} \text{MRE} &= 0.00469 \\ \text{MSRE}^{1/2} &= 3.02 \\ \text{MSE}^{1/2} &= 0.192 \end{aligned}$$

Case fipsil36: Spherical isotropic model (lag-class fitting) (SAM 92-865-40)

$$\begin{aligned}\beta_1 &= -2.558 \\ \beta_2 &= 1.804 \\ \beta_3 &= 0.059797 \\ \text{Range} &= 300.18 \\ \text{Sill} &= 1.5021\end{aligned}$$

Cross-validation statistics:

$$\begin{aligned}\text{MRE} &= 0.0035 \\ \text{MSRE}^{1/2} &= 1.47 \\ \text{MSE}^{1/2} &= 0.192\end{aligned}$$

In these fitted models, the estimated contrast between Zone 2 and the rock mass is in the range 0.05 to 0.07 obtained by Norman (1992a). The strength of the trend with depth ( $\beta_2$ ) is estimated to be about the same, or less than estimated by Norman. In the case of a lesser trend with depth, the constant part of the trend is estimated to be lower.

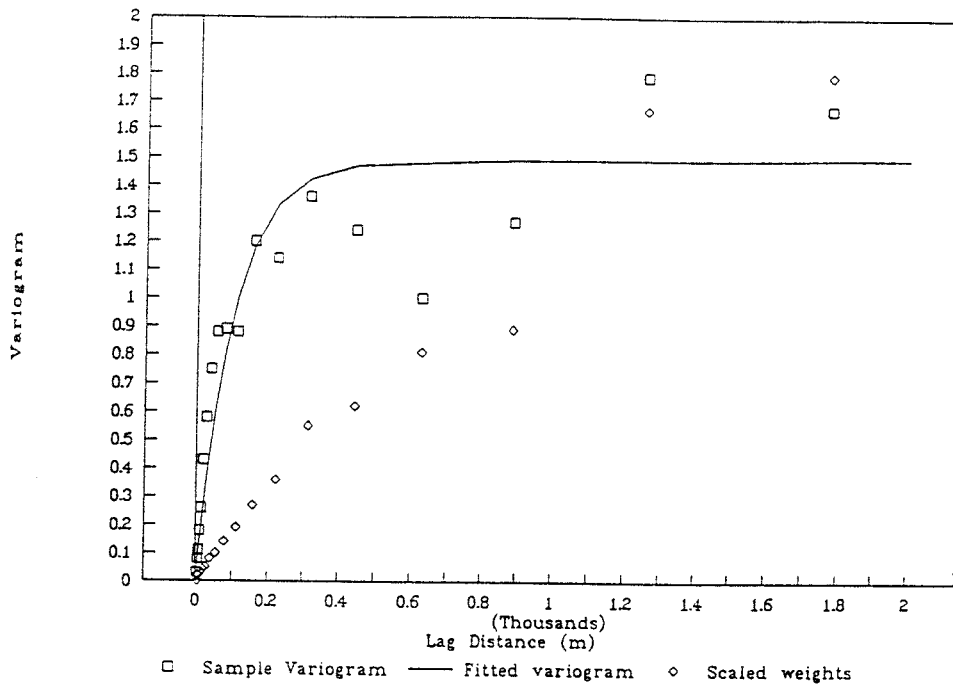
Interestingly, in both cases the lag-class fitting yields better models in terms of MRE and MSRE. The cross-validation statistics are generally less good than for the models estimated by Norman. The models estimated by direct fitting, in particular, have MSRE which is much too high.

Figures 4-6 and 4-7 show comparisons of these models with the sample semivariograms for the residuals. The best fit, visually, is given by the exponential model fitted using lag classes, which also happens to have the best cross-validation statistics. The spherical lag-class model is less good for the shorter lags.

Both of the direct-fitted models have sills which are much too low. Possibly this is a manifestation of non-robustness in the direct-fitting algorithm, due to a group of data pairs which have very strongly correlated residuals, after removing the trend. Unfortunately there are so many data that it is not feasible to produce a plot of  $y(x_i)y(x_j)$  for all data pairs, which could show the outliers which may be the source of the non-robustness.



Case: fipeil36



Case: fipeil36

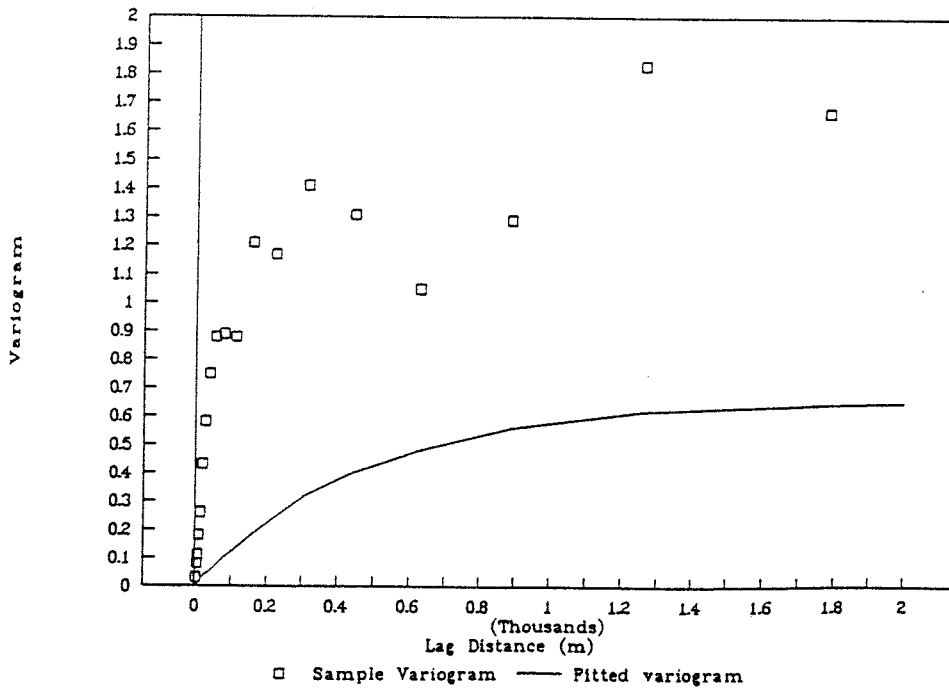
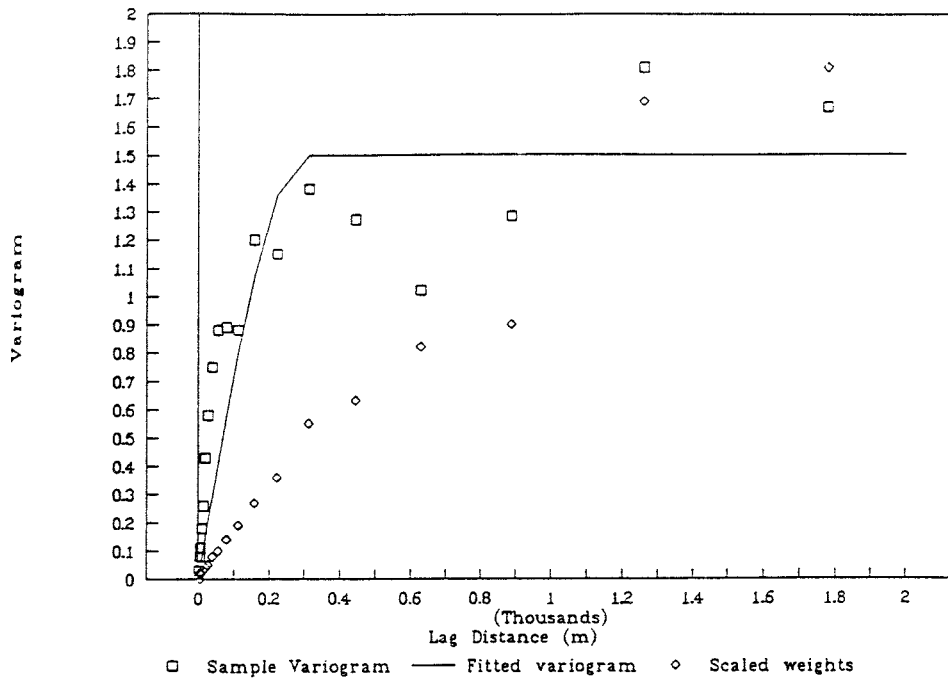


FIGURE 4-6ab  
FINNSJÖN POTENTIAL-TYPE MODEL,  
EXPONENTIAL, ISOTROPIC (lag, direct).

Case: fipsil36



Case: fipsin36

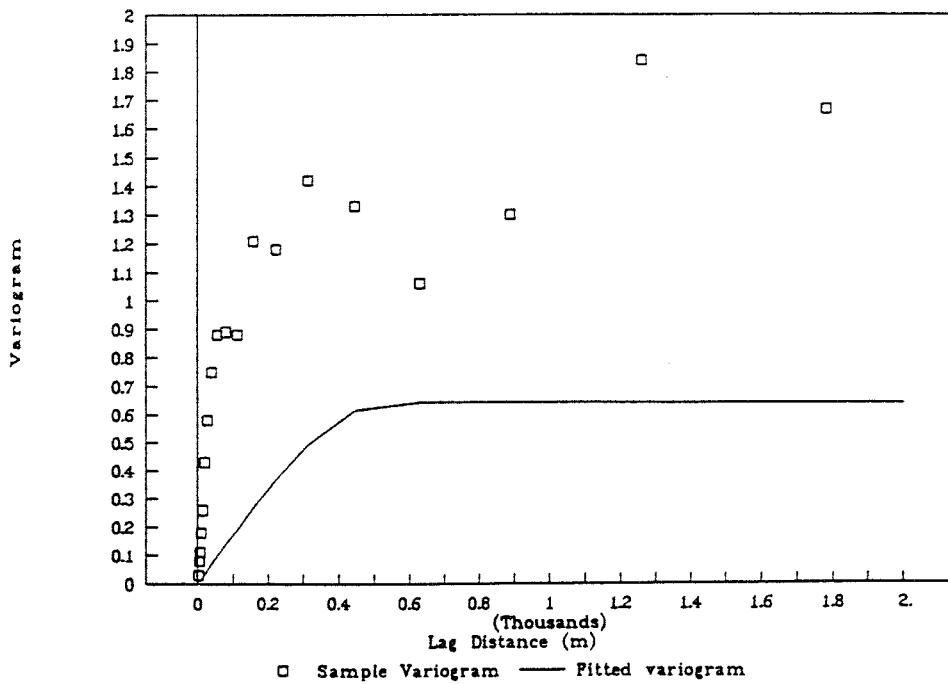


FIGURE 4-7ab  
FINNSJÖN POTENTIAL-TYPE MODEL,  
SPHERICAL, ISOTROPIC (lag, direct).

#### 4.2.2 Horizontally isotropic models

##### Case fipehl36: Exponential horizontally isotropic model (lag-class fitting) (SAM 92-865-034)

This run crashed after the second step of the grid-based search, due to undetermined causes. The best fit obtained from the first two steps was:

$$\begin{aligned}\beta_1 &= -1.660 \\ \beta_2 &= 2.253 \\ \beta_3 &= 0.121 \\ \text{Range} &= 98.5 \\ \text{Sill} &= 1.132 \\ \mathbf{G} &= \begin{matrix} 0.951 & 0 & 0 \\ 0 & 0.951 & 0 \\ 0 & 0 & 1.105 \end{matrix}\end{aligned}$$

Directional ranges:

$$\begin{aligned}\text{Horizontal range} &= 104 \text{ m} \\ \text{Vertical range} &= 89 \text{ m}\end{aligned}$$

No cross-validation statistics were calculated for this model.

##### Case fipehn36: Exponential horizontally isotropic model (direct fitting) (SAM 92-865-035)

$$\begin{aligned}\beta_1 &= -2.311 \\ \beta_2 &= 1.919 \\ \beta_3 &= 0.062 \\ \text{Range} &= 785.28 \\ \text{Sill} &= 1.4267 \\ \mathbf{G} &= \begin{matrix} 0.614 & 0 & 0 \\ 0 & 0.614 & 0 \\ 0 & 0 & 2.65 \end{matrix}\end{aligned}$$

Cross-validation statistics:

$$\begin{aligned}\text{MRE} &= 0.00298 \\ \text{MSRE}^{1/2} &= 1.10 \\ \text{MSE}^{1/2} &= 0.192\end{aligned}$$

Directional ranges:

$$\begin{aligned}\text{Horizontal range} &= 1279 \text{ m} \\ \text{Vertical range} &= 296 \text{ m}\end{aligned}$$

The direct-fitted, horizontally anisotropic exponential model has surprisingly large ranges in both vertical and horizontal directions. The cross-validation statistics are somewhat worse than the best isotropic, exponential model fitted using a potential-type trend. Figure 4-8 compares the fitted model with the semivariograms for different angular lag classes.

Case: fipehn36

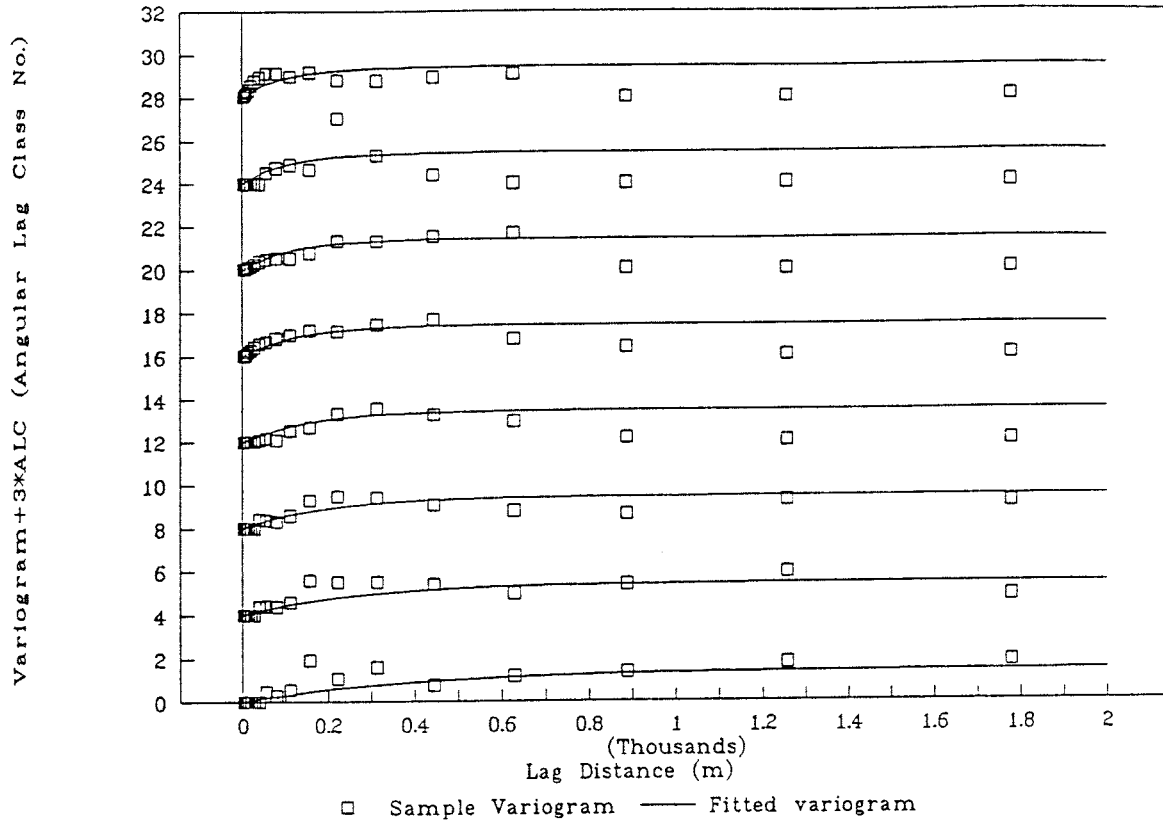


FIGURE 4-8  
FINNSJÖN POTENTIAL-TYPE HORIZONTALLY,  
ISOTROPIC EXPONENTIAL MODEL (direct fitting).

Case fipshl36: Spherical horizontally isotropic model (lag-class fitting) (SAM 92-865-038)

$\beta_1$  = -1.753  
 $\beta_2$  = 2.205  
 $\beta_3$  = 0.071  
 Range = 294.01  
 Sill = 1.1987  
 G =      0.499   0      0  
       0      0.499   0  
       0      0      4.02

## Cross-validation statistics:

MRE = 0.00205  
 MSRE<sup>1/2</sup> = 0.845  
 MSE<sup>1/2</sup> = 0.194

## Directional ranges:

Horizontal range = 589 m  
 Vertical range = 73 m

Case fipshn36: Spherical horizontally isotropic model (direct fitting) (SAM 92-865-039)

This run was killed after completing just 3 steps of the grid-based search, in 4 days of run time on the Convex. On the last step the IGLSE process for estimating  $\beta$  seemed to be rather unstable. The first steps of the grid-based search produced models with extreme anisotropy, e.g:

$\beta_1$  = -3.926  
 $\beta_2$  = 1.253  
 $\beta_3$  = 0.1126  
 Range = 414.5  
 Sill = 0.9703  
 G =      3130.   0      0  
       0      3130.   0  
       0      0      1×10<sup>-7</sup>

and

$\beta_1$  = -0.9755  
 $\beta_2$  = 2.616  
 $\beta_3$  = 0.7482  
 Range = 553.0  
 Sill = 1.378  
 G =      5×10<sup>-3</sup>   0      0  
       0      5×10<sup>-3</sup>   0  
       0      0      3×10<sup>-4</sup>

The model estimated by lag-class fitting, on the other hand, had a reasonable degree of anisotropy and fairly good cross-validation statistics. Figure 4-9 compares this model with the semivariograms for different angular lag classes.

Case: fipsh136

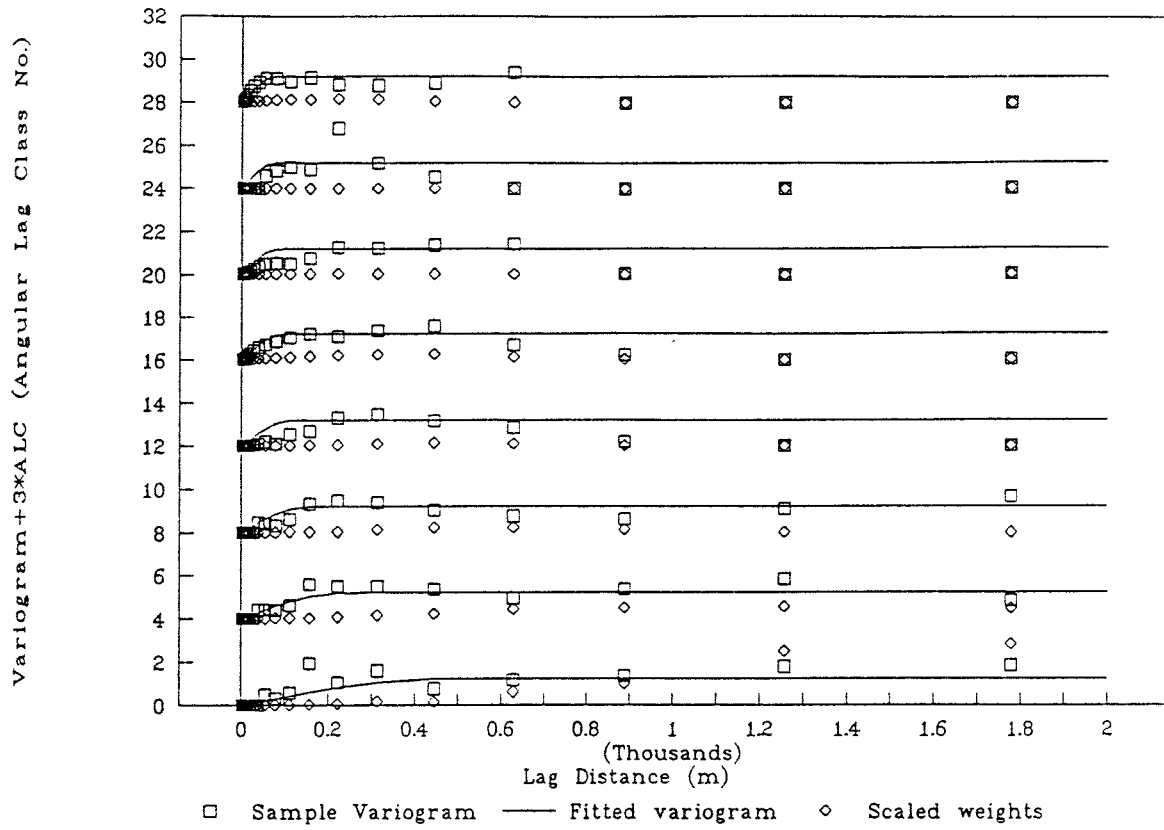


FIGURE 4-9  
 FINNSJÖN POTENTIAL-TYPE HORIZONTALLY,  
 ISOTROPIC SPHERICAL MODEL (lag-class fitting).

## 5. CONCLUSIONS AND RECOMMENDATIONS

### 5.1 Verification cases

The verification exercises described in Chapter 3 of this report confirmed the functionality of the algorithms for fitting simple isotropic, simple horizontally isotropic, and nested isotropic models.

The code was also successful in fitting nested isotropic models, in that the fitted nested semivariogram gave a good match to the sample semivariogram. However, the fitting of these models was found to be a somewhat difficult process. Firstly, a substantial amount of data is required to allow resolution of more than one component model. Even when the quantity of data is sufficient, the fitting algorithm may still, in some cases, produce a solution which represents only the dominant component of the nested model, due to the occurrence of local optima.

The verification exercises to test fitting of more complicated nested models, with anisotropic submodels, gave mixed results. Further verification exercises, and experiments with synthetic data, are needed to determine what type of data support is required for these models.

The verification performed thus far is mainly qualitative. Quantitative verification will require development and implementation of statistical tests for the significance of discrepancies between the sample semivariogram and the input model, for the simulated datasets which are used to test the fitting routines.

## 5.2 Demonstration using the Finnsjön dataset

The results obtained for the Finnsjön dataset confirmed several of the results and conjectures of Norman (1992a):

- The contrast between Zone 2 and the surrounding rock was found to be of approximately the same magnitude as estimated previously.
- The sensitivity of anisotropy estimates to arbitrarily chosen lag classes was confirmed by comparisons between the results of lag-class and direct fitting.
- The anisotropic models were generally worse, in terms of cross-validation statistics, than the corresponding isotropic models.

However, two of the extensions to the code which were made following that study gave disappointing results:

- The use of direct fitting, rather than arbitrary division of the data pairs into lag classes, was apparently less robust, and in general gave less good solutions in terms of the cross-validation statistics.
- The use of nested models gave better results in terms of goodness of approximation to the sample variogram. However, the models which were obtained were still not very good in terms of their cross-validation statistics.

The seemingly paradoxical result that higher-order models (*e.g.* nested or anisotropic) do not generally yield better cross-validation statistics than the simplest models (even though they incorporate more adjustable parameters), is explainable by the fact that the optimum model in terms of cross-validation statistics is not necessarily coincident with the least-squares match to the sample covariance.

The demonstration cases included a more generalized anisotropic model (with principal axes of anisotropy aligned with the coordinate axes). The results were quite close to those for the horizontally isotropic models, indicating that the covariance is approximately isotropic in the horizontal plane.



### 5.3 Practicality of fitting algorithms and techniques

The **grid-based search** algorithm was found to provide a useful, automatic way of exploring the parameter space. In many of the verification and demonstration cases, a grid-based search yielded multiple solutions representing local optima, in terms of the least-squares criteria.

In a few cases multiple local optima were in fact found by the grid-based search, confirming the need for a thorough exploration of the parameter space to give a better chance of locating the global optimum. Unfortunately the runtime is proportional to the number of starting points in the search. Hence for the more complex models, as the number of model parameters increases there are limits to how thoroughly the parameter space can be investigated.

**Direct fitting** is apparently not practical for nested anisotropic models, and the large datasets (ca. 4000 data points) which are required to support them. For this scale of problem, lag classes must be used (if the runs must be limited to, say, 20 CPU-hours on the Convex).

Direct fitting is also not practical when trend functions and covariance functions are being estimated simultaneously (IGLSE), for covariance models more complicated than simple isotropic or horizontally isotropic.

A comparison of the results obtained for lag-class and direct fitting shows that often the models estimated by lag-class fitting are better kriging predictors, as measured by the cross-validation statistics. It is speculated that properly (or fortuitously) chosen lag classes and weighting schemes may, in effect, give more robust estimates of the covariance functions. The direct fitting method may be influenced by outlier data pairs. The effects of these outliers would be diminished for lag-class fitting would be diminished by the averaging within lag classes.

The apparent non-robustness of direct fitting is a major barrier for objective inference of site models, in view of the sensitivity of fitted models to lag class definition. Possible solutions which might be investigated include:

- Optimization with respect to the log-likelihood of the kriging errors for a model, as described by Samper & Neuman (1989), rather than fitting to the sample semivariogram.
- Incorporation of robust estimation techniques in the direct-fitting algorithm.

The first of these has the further advantage of directly optimizing the crucial aspect of the covariance model (namely its goodness as a kriging predictor), which is directly related to the idea of measuring the goodness of the model in terms of cross-validation statistics. Most of the subroutines needed to implement this approach have already been developed, for the calculation of cross-validation statistics. However the practicality of the method for large datasets (comparable to that for Finnsjön) is questionable, since each step in the estimation requires a new solution of the kriging equations.

Robust estimation techniques can be implemented fairly easily in the existing code. The simplest approach is to convert from the  $L_2$  norm (*i.e.* the least-squares criterion), to an  $L_1$  norm (*i.e.*, the

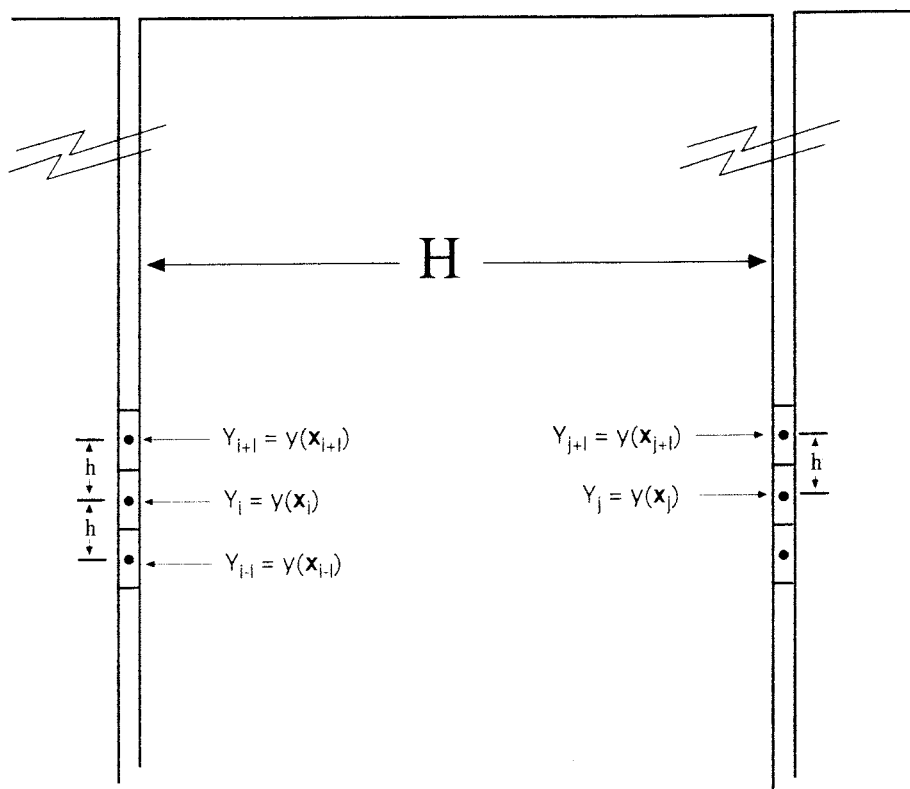


FIGURE 5-1  
**INTRAHOLE AND  
 INTRAHOLE DATA PAIRS**

sum of the absolute errors). However this gives an objective function with discontinuous first derivatives, which might produce instability in the fitting. A better solution may be to instead minimize the sum of some robust function of the residuals, e.g. the bisquare function:

$$f(r) = \begin{cases} (1-r^2)^2, & |r| \leq 1 \\ 0, & |r| > 1 \end{cases} \quad (5-1)$$

where  $r$  is the residual for a given lag, normalized, say, by the standard deviation of the residuals.

The accuracy of the semivariogram fits could perhaps be improved by a more appropriate weighting scheme for between-hole lags. The sample semivariograms for the synthetic datasets used in verification show good agreement with the input models for short lags, but poor agreement for the longer lags, despite the fact that there are many more data pairs (*i.e.* samples) for the longer lags. If the simulation routines are not grossly in error for the longer lags, then the observed disagreement can only be explained as being due to an insufficient number of *independent* samples at long lags.

The problem seems to be due to the strong clustering of the measurements along boreholes. The increments of the log conductivity for lags from two adjacent intervals in a borehole (see Figure 5-1 for notation) have covariance:

$$E[(y_{i+1} - y_i)(y_i - y_{i-1})] = 2C(h) - C(2h) \quad (5-2)$$

which is typically of the same order as  $C(h)$ , the covariance of the function which is being estimated for the intrahole lag  $h$ . However, the between-hole increments for two adjacent sections have covariance:

$$E[(y_{i+1} - y_{j+1})(y_i - y_j)] = 2C(h) - 2C(H) \quad (5-3)$$

which, for  $H \gg h$ , is typically many times larger than  $C(H)$ , the covariance being estimated for the interhole lag  $H$ . In other words the short-range correlation between clustered data pairs obscures the relatively small, long-range covariance, so that many more measurements are needed to estimate the long-range covariance correctly.

In INFERENS 1.1, all data pairs are arbitrarily assigned equal weight in direct fitting. A weighting scheme which takes into account the strong correlation of neighboring interhole data pairs, relative to the magnitude of covariance for those lag distances, would give more appropriate emphasis to the intrahole lags.

**Synthetic dataset generation** is a new capability which was developed to facilitate code verification. This capability can readily be applied to a systematic study of data requirements for covariance model estimation, *i.e.* to determine the sampling density and/or quantity of data necessary to estimate a given type of covariance model, to within a given tolerance.

## 6. ACKNOWLEDGMENTS

The original version of INFERENS was developed by Sven Norman and Lars Lovius. Although revisions were made in the current study, many of these were rather superficial. The functionality of the code still is mainly due to a core of numerical algorithms which were cleverly derived and implemented by Sven and Lars.

The author wishes to thank Sven, furthermore, for his copious help in understanding the intricacies of this code, and for unravelling the author's confusion in several instances.

Nils Kjellbert is thanked for his help with programming PROPERly on the Convex, and for his ideas regarding the meaning of the eventual results.

Thanks are extended to Anders Ström, in particular, for his many helpful suggestions, his assistance on the Convex, and especially for his patience, throughout what has been a rather long effort.

## 7. REFERENCES

Efron, B., 1978. *The Jackknife, the Bootstrap, and Other Reampling Plans*, monograph published by the Society for Industrial and Applied Mathematics, Philadelphia, Pennsylvania, USA.

Geier, J., 1993. INFERENS Version 1.1 User's Manual, GGAB project memorandum prepared for SKB, Stockholm.

Moye, D.G., 1967. "Diamond drilling for foundation exploration," *Civil Engineering Transactions*, pp. 95-100.

Norman, S., 1992a. "Statistical inference and comparison of stochastic models for the hydraulic conductivity at the Finnsjön site", SKB Technical Report 92-08, SKB, Stockholm.

Norman, S., 1992b. "INFERENS User's Manual", STARPROG AB draft memorandum prepared for SKB, Stockholm.

Samper, F.J. & S.P. Neumann, 1989. "Estimation of spatial covariance structures by adjoint state maximum likelihood cross validation, 1. Theory," *Water Resources Research*, Vol. 25, No. 3, pp. 351-362.

**Technical Reports**  
**List of SKB Technical Reports 1993**

TR 93-01

**Stress redistribution and void growth in  
butt welded canisters for spent nuclear  
fuel**

B L Josefson<sup>1</sup>, L Karlsson<sup>2</sup>, H-Å Häggblad<sup>2</sup>

<sup>1</sup> Division of Solid Mechanics, Chalmers  
University of Technology, Göteborg, Sweden

<sup>2</sup> Division of Computer Aided Design, Luleå  
University of Technology, Luleå, Sweden

February 1993

TR 93-02

**Hydrothermal field test with French  
candidate clay embedding steel heater in  
the Stripa mine**

R Pusch<sup>1</sup>, O Karnland<sup>1</sup>, A Lajudie<sup>2</sup>, J Lechelle<sup>2</sup>,  
A Bouchet<sup>3</sup>

<sup>1</sup> Clay Technology AB, Sweden

<sup>2</sup> CEA, France

<sup>3</sup> Etude Recherche Materiaux (ERM), France

December 1992

TR 93-03

**MX 80 clay exposed to high temperatures  
and gamma radiation**

R Pusch<sup>1</sup>, O Karnland<sup>1</sup>, A Lajudie<sup>2</sup>, A Decarreau<sup>3</sup>,

<sup>1</sup> Clay Technology AB, Sweden

<sup>2</sup> CEA, France

<sup>3</sup> Univ. de Poitiers, France

December 1992

TR 93-04

**Project on Alternative Systems Study  
(PASS)**

Final report

October 1992

TR 93-05

**Studies of natural analogues and  
geological systems.**

**Their importance to performance  
assessment.**

Fredrik Brandberg<sup>1</sup>, Bertil Grundfelt<sup>1</sup>, Lars Olof

Höglund<sup>1</sup>, Fred Karlsson<sup>2</sup>,

Kristina Skagius<sup>1</sup>, John Smellie<sup>3</sup>

<sup>1</sup> KEMAKTA Konsult AB

<sup>2</sup> SKB

<sup>3</sup> Conterra AB

April 1993

TR 93-06

**Mineralogy, geochemistry and  
petrophysics of red coloured granite  
adjacent to fractures**

Tomas Eliasson

Chalmers University of Technology and University  
of Göteborg, Department of Geology, Göteborg,  
Sweden

March 1993

TR 93-07

**Modelling the redox front movement in a  
KBS-3 nuclear waste repository**

L Romero, L Moreno, I Neretnieks

Department of Chemical Engineering,

Royal Institute of Technology, Stockholm, Sweden

May 1993

TR 93-08

**Äspö Hard Rock Laboratory  
Annual Report 1992**

SKB

April 1993